

## **Objectives of Study**

This report is a structural study of the static behavior of the Pine Bluff Covered Bridge, built with the Howe truss. A principal objective of this study was to quantify the effect of tightening rods, in order to evaluate the effectiveness of Howe's proposed prestressing technique. Additional objectives were to quantify the static behavior of the Pine Bluff Bridge under dead load, prestressing, live load, shrinkage, and creep, and to provide guidance for assessment, rehabilitation, and maintenance of this type of truss.

## **Scope of Study**

The main features of Howe trusses and of the Pine Bluff Bridge in particular were determined from available documents and on-site measurements. A review of wood properties, in particular, the temporal properties of shrinkage and creep, is presented. Common mechanical and physical property values were used for structural analyses of the bridge. Specific information on the temporal properties of wood were gathered in order to evaluate the effects of shrinkage and creep on the truss, in particular on the initial prestressing state. Common mechanical and physical property values were used for the structural analyses of the bridge. Specific information on the temporal properties of wood was researched in order to evaluate the effects of shrinkage and creep on the truss, in particular on the initial prestressed state.

Tests with tightening rods were done in order to measure strains and, consequently, prestressing forces produced in the elements by using Howe's prestressing technique. Tests were completed using a truck of known weight that traversed one span. Data on the actual behavior of the bridge was collected so a comparison could be done between the bridge's behavior in prestressed and un-prestressed conditions.

Finite element analyses of the Pine Bluff Bridge, using several linear elastic, plane frame models, were performed to study the static behavior of the bridge. The bridge was studied under the action of dead load alone; prestressing; moving, concentrated live loads; and a uniformly distributed live load.

## **Principal Observations**

The experimental studies showed that the order of magnitude of the tensile forces produced in the rods by tightening nuts to prestress them was about 6-7 kips for each rod of a vertical element (12-13 kips for the whole vertical element).<sup>1</sup> Experimental influence lines for certain element forces and vertical displacements were plotted.

The portion of this study involving the viscous behavior of wood revealed a scarcity of generally applicable data. In practice, simple displacement amplification is often used to

---

<sup>1</sup> One kip equals a 1,000-pound force.

take these temporal effects into account. For the analysis of prestressed systems, there is a need for improved viscous models of wood behavior.

The numerical studies of the static behavior of Pine Bluff Bridge showed that the maximum axial stresses under dead load in the elements were about 200 pounds per square inch (psi). Also, stresses from bending moments were an order of magnitude smaller than those from axial forces, and shear forces in the members were almost zero. The maximum vertical displacements of the analytical model of the Pine Bluff Bridge under dead load were equal to 0.56 inches without the effect of prestressing (the counters were inactive), and to 0.39 inches with the action of counterbraces. A considerable additional stiffness (+30 percents) was therefore obtained by activating the counters.

Regarding the prestress, the action of tightening a rod primarily affects the two panels adjoining the rod. Prestressing causes a very small upward displacement of the truss; therefore, it only slightly relieves the dead load forces from the falsework. The truss should be prestressed with the falsework removed and the dead load already active, although the tightening of the rods could require more effort.

Influence lines of some main diagonals and counterbraces for a moving live load are shown. They were used to evaluate the minimum concentrated live load that would cause slackness in the diagonal elements of the truss. This live load is about 6.5 tons to loosen the central main diagonals in the un-prestressed case, and about 18 tons to loosen the counterbraces of the panels adjacent to the end ones with the bridge prestressed and the counters active. The same elements were loosened, in the two bridge conditions, for uniformly distributed live loads of about 57 pounds per square foot ( $\text{lb}/\text{ft}^2$ ) and  $74 \text{ lb}/\text{ft}^2$  on half span of the bridge. These critical live loads were compared with design live loads used at the end of the nineteenth century.

Longitudinal wood shrinkage, being non-uniformly distributed on the truss elements (the vertical wrought iron rods do not shrink), caused large changes in stresses in the elements and a significant loss of prestress in the counterbraces. The first critical counters that became slack were those in the panels adjacent to the end ones. Shrinkage also causes downwards displacements. The effect of tangential and radial shrinkage at nodes cannot be evaluated with the models used here. More detailed models would be needed to predict them. However, it should be noted that when the cast-iron bearing shoes are properly made, there is no bearing on the horizontal chords and the joints should be dramatically affected by tangential and radial shrinkage.

Creep also causes a loss of prestress in the counterbraces, but may or may not be sufficient to cause slackness. The critical counters that can become slack are those closest to the span ends. However, to predict the time-to-slackness, a viscous stress-strain model for wood that takes into account the change in stresses with time would be needed. Finally, a comparison of numerical results and experimental measurements is given. The results reveal that the experimental stiffness of Pine Bluff Bridge was lower

than numerically predicted. Some hypotheses to explain the lower actual stiffness are presented.

Linear, elastic plane frame models can be adequate to predict short term behavior of wooden trusses, but they need to be calibrated through experimental testing on a real structure, as proven in the case of Pine Bluff Bridge. Linear, elastic models with prescribed shrinkage and/or creep strains can only provide a general idea of whether slackness will occur and where, but cannot give more detailed information on time-to-slackness. However, from the results of the analyses performed, it is clear that for a Howe truss, a periodic re-tightening of wrought iron rods is needed, more often during the early stages of the bridge's life, to maintain the original bridge behavior.

### **Construction of the Pine Bluff Bridge and Original Details**

The Pine Bluff Bridge has two spans of Howe trusses with a total length of 211'. The pier and abutments of the bridge are of cut stone laid with mortar and jacketed with concrete. The bridge has a sheet metal roof and vertical siding painted red, with two windows, one on each side of the bridge. The portals are straight with 45-degree fillets in the top corners, a typical Britton detail.



**Fig. 1: External view of the Pine Bluff Bridge from north, field photograph.**

The lumber used on the bridge has not been definitively established. It has been hypothesized, from other bridges in the area, that it may be Michigan pine, a kind of white pine. For the decking, harder woods like red oak were generally used at that time. Red oak was available in many areas of Indiana, and it was extensively used for floor systems, although there were some instances of it being used for trusses. The floor was

laid in two layers, one orthogonal to the bridge length and the other placed lengthwise over the orthogonal layer.<sup>2</sup>



**Fig. 2: Internal view of the Pine Bluff Bridge, field photograph.**

The width of each panel is about 120” from vertical element to vertical element. The counterbraces have dimensions increasing from the ends to the center of the span. Their sections change from 6x6” in the end panels to 8x8” in the central ones. Conversely, the dimensions of the main diagonals and vertical rods decrease from the ends of the span to mid-span. The main diagonals are each made of two timbers that vary in dimension from 8x9” in the end panels to 6x8” in the central panels. Diagonals and counters are bolted together at mid-length. The vertical elements are composed of two iron rods each that change in diameter from 1” each at the center to 1.5” at the span ends. They pass through bearing blocks (see Figure 3), which are triangular cast iron prisms that match the width of the chords. The diagonal elements of the truss, which are cut orthogonally to their length, bear against the inclined faces of the bearing blocks. The blocks, in turn, bear against, but are not pinned or bolted to, the upper chord. A small shear key prevents each block from slipping along the chord.

---

<sup>2</sup> W.M. Weber, *Covered Bridges in Indiana* (Midland, MI: Northwood Institute, 1977); and G.E. Gould, “Indiana’s Covered Bridges Built by Inventive and Skillful Craftsmen” *Outdoor Indiana* (February 1978), 4-18.



**Fig. 3: Bearing block between diagonal elements and the upper chord, field photograph.**

Unlike Howe's later, solid design (1846 patent), these bearing blocks are hollow castings, and the high bearing forces at their ribs tended to crush the wood in the chords (see Figures 4 and 5). The use of a hollow bearing block on the Pine Bluff Bridge could be due to the relative inexperience of Britton in 1886. The early Britton bridges were not as well made or precise in detail as his later ones.<sup>3</sup>

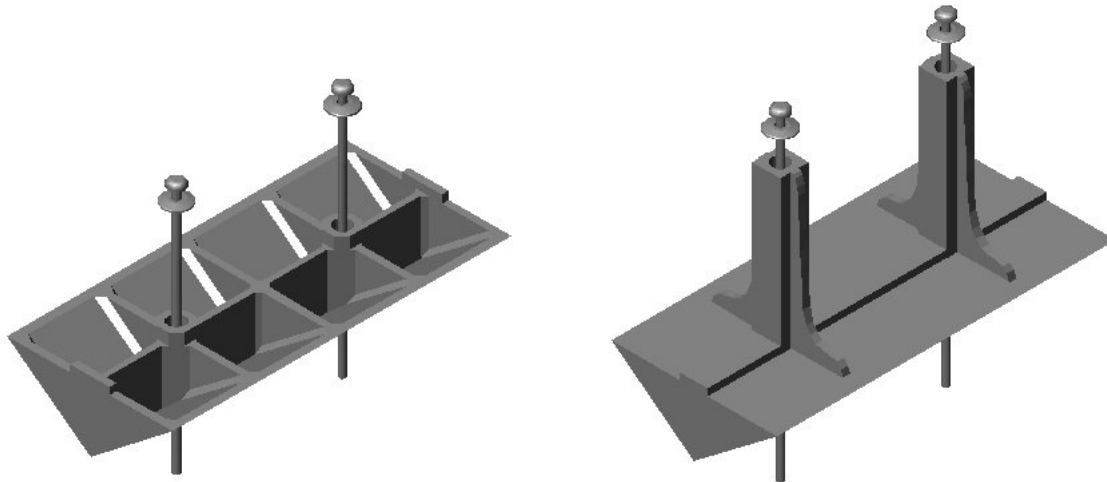


**Fig. 4: Measured hollow bearing block in Pine Bluff Bridge (left) and later solid bearing block design to prevent the crushing of chords (right).**

---

<sup>3</sup> Weber, *Covered Bridges in Indiana*.

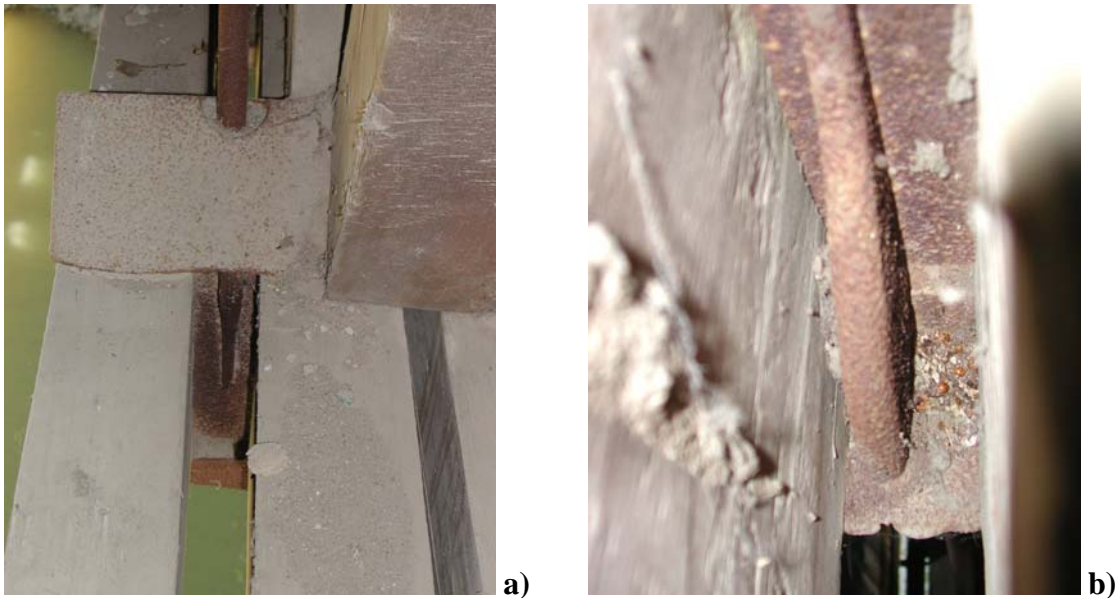


**Fig. 5: Later bearing block (a) and detail of stiffening flange in bearing block (b), Dick Huffman Bridge, Putnam County, IN, field photograph.**

The top and the bottom chords are made of four timbers each with overall section areas of 203 and 233 square inches, respectively. Simple rectangular wooden shear connectors splice the upper chord, while the lower chord has both rectangular shear blocks and a wooden splice (see Figures 6 and 7).<sup>4</sup>



**Fig. 6: Upper chord splicing (left) and lower chord splicing (right), field photograph.**

---

<sup>4</sup> For a discussion of Britton’s evolution in detail construction and chords splicing, see: J.M. Vlach, “Daniels and Britton, Master Bridge Builders,” *Indiana Covered Bridge Society Newsletter* 9, no. 4 (October 1972): 1-3.

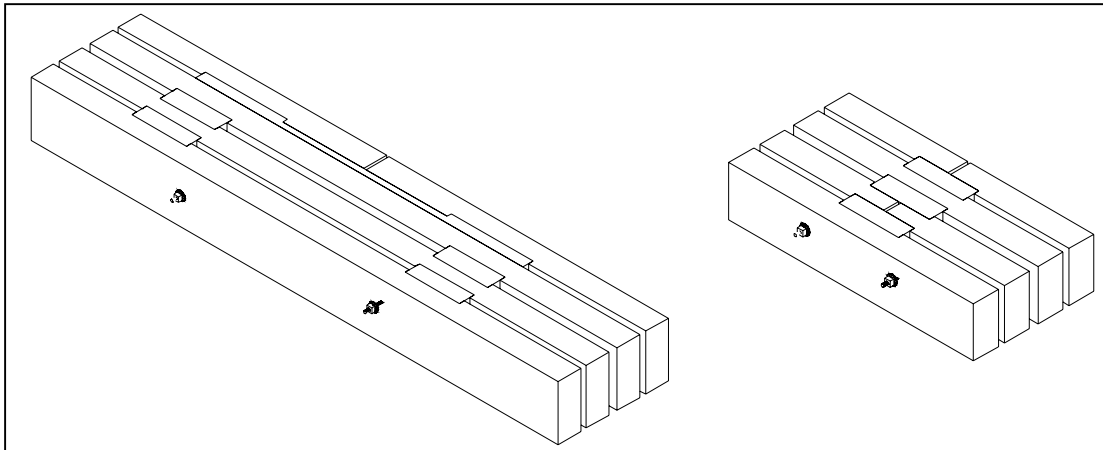


**Fig. 7: Chord splicing: lower chord (left), upper chord (right).**

Small iron angles support the upper lateral bracing system. Each cross brace has an iron rod bolted through the chord. The lower lateral bracing is connected to the lower chord in a similar manner (see Figure 8a). Figure 8b shows a general view of the decking and lower lateral bracing from underneath the bridge.



**Fig. 8: Lower lateral bracing joint (a) and general view of the decking and lower lateral bracing from beneath the bridge (b), field photographs.**

The Pine Bluff Bridge is a classic Howe truss; however, Britton's use of hollow bearing blocks, long after the expiration of Howe's and Piper's patents for castings that prevented crushing of the chords, is surprising.

### **Subsequent Repairs of the Pine Bluff Bridge**

The Pine Bluff Bridge has undergone various repairs over the years, and different consultants have been retained by Putnam County to assess the bridge's condition and propose repairs. From county reports, it is known that a decennial re-tightening of the

rods began in the nineteenth century. One of the first alterations, which involved concrete repairs to the substructure, was probably made in 1917.



**Fig.9: View of an abutment showing the concrete jacketing of the original masonry structure and concrete pillars for lifting-up the bridge, field photograph.**

The 1974 inspection report revealed the presence of badly twisted floor beams that were too light to support truck traffic. Loose diagonals, rotted and crushed bearing connections, and a sag in the east span were also noted. The report recommended replacing the deteriorated components (bearings and floor beams) and limited the allowable live load by erecting “one lane bridge” and “no trucks” signs. The diagonal slackness was said to be partly caused by the crushed bearing blocks at the pier, but no mention was made of the possibility of tightening the rods to counteract the looseness.<sup>5</sup>

In 1983, the county decided to make additional repairs to the bridge, but insufficient funds were available until 1986, when work finally started. The repairs focused on the floor system (see Figure 10), where the existing, small floor beams—probably 3x12” stringers spaced about every 2’, possibly three or four per panel—were replaced with two 11x12” glue-laminated (glulam) beams per panel. These were installed close to the posts, in non-symmetrical arrangement on the lower chord (at about 1/5 and 7/10 of the panel length). Similar repairs have been made on other Putnam County bridges. The roof has also undergone replacement.

---

<sup>5</sup> Butler, Fairman & Seufert, Inc., *Bridge Inspection Report, Putnam County, IN*, 1974.

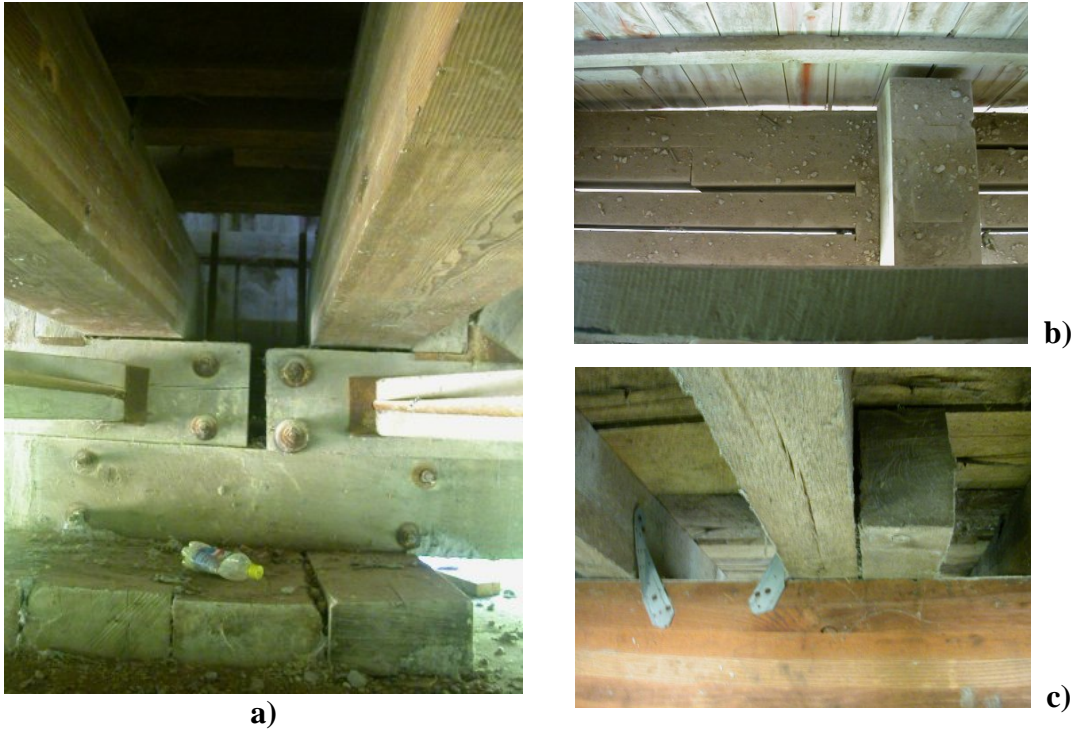


**Fig. 10: Deck bearing beams at pier support (a); glulam beam on the lower chord, view from above (b); and detail of a connection between the new deck bearing beams and the old floor beams (c), field photographs.**



**Fig.11: View of the replaced roof (left) and connection between rafters and upper chord (right), field photographs.**

**Present Condition of the Pine Bluff Bridge (as of 2002)**

An on-site inspection of the bridge from June 16 to June 18, 2002, found all the counterbraces loose and some vertical rods slack. Figure 12 shows the upper end of a counterbrace that is clearly loose. Currently, the roof rafters are simply supported on the upper chord, without ties. The deck has poor vertical alignment with the road, especially at the southern approach. Unless settlement of the south abutment occurred, it is very probably that the vertical misalignment is due to road level changes during more than one hundred years of use. Regardless of cause, this situation causes every vehicle entering the bridge to impose an unnecessary dynamic load on the structure, the severity of which increases with vehicle speed. Reducing vehicle approach speeds, if possible, would substantially reduce the dynamic effects, at least until the road surface can be better aligned with the bridge.

The lower chord timbers do not appear to have particular problems with rot, but dirt at the support and on the lower chord should be removed to minimize moisture retention.<sup>6</sup> On the upper chord, the bearing blocks have slipped about half an inch, in the direction from the main diagonal to the counter. This phenomenon, although limited, is very typical of this kind of joint.

Some insect boreholes were noted, particularly in the diagonal elements of the truss. Figure 13 shows an example of this damage.



**Fig. 12: Loose counter and slipping of the bearing block on the upper chord, field photograph.**



**Fig.13: Insect infestation on a diagonal element, field photograph.**

## **STATIC BEHAVIOR OF THE PINE BLUFF BRIDGE**

<sup>6</sup> E.E. Wallace and J.W. Clark, *Wood Bridges: Decay Inspection and Control* (Washington, DC: Forest Service, U.S. Department of Agriculture, 1979).

### **Issues Concerning the Analysis of Pine Bluff Bridge**

There are a number of issues surrounding the analysis of the bridge. First of all, the initial states of stress obtained by tightening the nuts on the wrought iron rods have to be clarified. The actual effectiveness of the prestressing technique with time has to be verified. When modeling the structure, therefore, the presence of prestressing forces and their effectiveness (presence of active stiffening counterbraces) or ineffectiveness (inactive counterbraces, with the bridge behaving as if they did not exist) has to be taken into account. A short-term analysis of the bridge can be carried out bearing in mind that, due to the high temporal dependency of the stress-strain behavior of wood, there also will be long-term effects caused by shrinkage and creep. If an analysis of shrinkage and creep effects is undertaken, remembering that they affect only wood and not iron, some simplifying hypotheses can be accepted. In two-dimensional models, only the effects of longitudinal shrinkage can be examined. Reasonably accurate strains due to creep can be calculated by assuming that the stresses in the truss members are constant.

### **Finite Element Analysis of Pine Bluff Bridge**

The Pine Bluff Bridge structural behavior was predicted by computer analysis of two-dimensional, linear elastic-frame models, using a commercially available structural analysis program.<sup>7</sup> A two-dimensional analysis was performed, based on experience to indicate that this would be sufficient to reveal the structural behavior. A frame model was used because of the continuity of the chords. In the models, the structure was represented by discrete elements, joined at nodes. In the case of a two-dimensional frame, each node has three independent components of displacement (degrees of freedom), i.e. two perpendicular displacements and one rotation.

Two models of the Pine Bluff Bridge were used as shown in figures 14 and 15. Model A (Figure 14) assumed the counterbraces were loose. This model reflects the actual condition of the bridge, as verified during the on-site inspection. Model B (Figure 15) assumed that, because of prestressing, the counters could act both in tension and in compression. The frame models were symmetric, so, as expected, symmetric loading conditions caused symmetric responses of the models.

Because of the similar nature of the two spans, an analysis of one truss would adequately represent the other as well. The panel points were arbitrarily numbered from west to east, and these the two figures represent the north truss of the east span. The member naming scheme derives from the numbers of the start and end nodes of each element.

---

<sup>7</sup> SAP 2000 NonLinear Version 6.11 for Windows, from Computer and structures, Inc., Berkeley, California



Element	Type	Length (in)	Area (in <sup>2</sup> )	Moment of inertia in plane (in <sup>4</sup> )	Section modulus in plane (in <sup>3</sup> )
L0L1, L1L2, L2L3, L3L4, L4L5	lower chord	120	232.9	2566	446
U0U1, U1U2, U2U3, U3U4, U4U5	upper chord	120	202.5	1687	337
L1U0	counter	229	36	108	36
L2U1, L3U2	counter	229	48	144	48
L4U3	counter	229	56	228	65
L5U4	counter	229	64	341	85
L0U1	diagonal	229	144	768	192
L1U2	diagonal	229	128	682	170
L2U3, L3U4	diagonal	229	112	457	130
L4U5	diagonal	229	96	288	96
L0U0, L5U5	vertical rod	195	1.57	0.098	0.196
L1U1	vertical rod	195	3.53	0.497	0.663
L2U2	vertical rod	195	3.08	0.377	0.539
L3U3	vertical rod	195	2.53	0.255	0.402
L4U4	vertical rod	195	1.99	0.157	0.28

**Table 1: Section properties of the truss elements.**

Concrete jacketing strengthened the original stone bridge abutments and pier. A site inspection of the bridge revealed that the spans were simply supported on wooden beams (four per each bottom chord). At the abutments these beams are fixed in concrete. These supports (see Figure 16) can resist not only vertical displacements but also horizontal ones and were therefore modeled as pins. On the contrary, at mid-span, the wooden truss is actually simply supported on beams on the central pier and some degree of horizontal displacement is allowed. These supports were thus modeled as roller-type connections.



**Fig. 16: Detail of the supports at the abutment (left) and at mid-span on the pier (right), field photographs.**

For the analysis, “white pine” material was assumed with the following elastic properties:

Modulus of elasticity,  $E = 1.2 \times 10^6 \text{ lb/in}^2$   
Poisson’s ratio,  $\nu = 0.33$

Wrought iron was assumed to have the following properties:

Modulus of elasticity,  $E = 2.8 \times 10^7 \text{ lb/in}^2$   
Poisson’s ratio,  $\nu = 0.3$   
Yield stress,  $f_y = 33000 \text{ lb/in}^2$

Both models A and B were used for analyzing the following loading cases:

1. dead load of the bridge
2. live load applied at different panel points
3. prestressing loads obtained by tightening the nuts
4. dead load, with prestressing and live loads applied at different panel points
5. dead load, with prestressing and effects from shrinkage and creep in the wooden members.

### **Analysis of the Pine Bluff Bridge under Dead Loads**

The structure’s dead load was calculated from the member properties, assuming a weight per unit volume equal to  $24.5 \text{ lb/ft}^3$  for the white pine of the truss,  $44 \text{ lb/ft}^3$  for the red oak assumed for the deck construction,  $484 \text{ lb/ft}^3$  for the wrought and cast iron elements. The analytical program automatically computed the weights of the truss members, however, a multiplier of 1.1 was applied to the truss weight to compensate for the miscellaneous wooden and metal elements. One-half of the deck and the roof weight were distributed to

each truss. The dead load of the roof was applied as a uniform load of 61.3 lb/ft on the upper chord, while on each lower chord element the dead load of the siding was applied as a concentrated load on the panel points equal to 385 lb, and the dead load of the deck was applied as two concentrated loads of 1400 lb each, at about 2/10 and 7/10 of each element length. A summary of the total dead loads of the Pine Bluff Bridge is listed in Table 2.

<b>WEIGHT OF THE TRUSS</b>						
Element:	upper chord	lower chord	vertical rods	diagonal	counter	cast iron bearing shoe
area (in <sup>2</sup> )	202.5	232.9	1.2	118.4	50.4	-
length (in)	120	120	210	229	229	-
weight (lb)	340.2	391.2	70.0	379.5	161.6	115.7
quantity/panel	1	1	2	1	1	2
weight/panel (lb)	340.2	391.2	140.0	379.5	161.6	231.4
<b>Weight per panel of the truss (lb)</b> (self weight)				<b>1644</b>		
<b>WEIGHT OF THE ROOF</b>						
Element:	rafters	Battens	crossing rod	diagonal brace	metal sheet	
area (in <sup>2</sup> )	5.25	2.50	0.79	36	142*	
length (in)	170	120	242	227	-	
weight (lb)	12.5	4.2	53.2	114.4	2.5**	
quantity/panel	5	13	0.5	1	-	
weight/panel (lb)	62.5	54.6	26.6	114.4	355	
<b>Weight per panel of the roof (lb)</b> (concentrated load on upper panel points)				<b>613</b>		
<b>WEIGHT OF THE DECK</b>						
Element:	bearing beams	floor beams	Planks	crossing rod	diagonal brace	
area (in <sup>2</sup> )	132	33	480	0.79	36	
length (in)	240	120	190	242	227	
weight (lb)	633.6	103.0	2371.2	53.2	212.5	
quantity/panel	1	7	0.5	0.5	1	
weight/panel (lb)	633.6	720.7	1185.6	26.6	212.5	
<b>Weight per panel of the deck (lb)</b> (2 concentrated loads of 1389.5 lb on the lower chord)				<b>2779</b>		
<b>WEIGHT OF THE SIDING</b>						
Element:	planks		hor. Int		Parapet	
area (in <sup>2</sup> )	120		10.5		17	
length (in)	170		120		120	
weight (lb)	285.6		17.6		28.6	
quantity/panel	1		4		1	
weight/panel (lb)	285.6		70.6		28.6	
<b>Weight per panel of the siding (lb)</b>				<b>385</b>		

(concentrated load on lower panel points)	
<b>Total weight of a bridge span:</b>	<b>108.4 (kips)</b>

**Table 2: Weight (dead load) of the Pine Bluff Bridge.**

Figure 17 shows the axial forces occurring in models A and B when subjected to their corresponding dead loads. The sign convention selected indicates forces producing tension in members as positive and forces producing compression in members as negative.

In both models, the chords have significant axial forces, compression in the upper chord and tension in the lower chord, which increase from the ends to the center of the bridge span. For both models and for both chords, the absolute value of the maximum axial forces was about 43 kips. The vertical and diagonal elements have increasing axial forces from the mid-span to the ends of the bridge. Bridge constructors seem to have understood this general behavior, as they often reduced the sectional areas of diagonals and posts toward the center of the bridge spans.

For all the elements, the maximum absolute values of bending moments and shear forces are reached in members close to the bridge ends (see respectively Figures 18 and 19). A summary of the forces in the main elements of the truss models A and B can be found in Table 3.

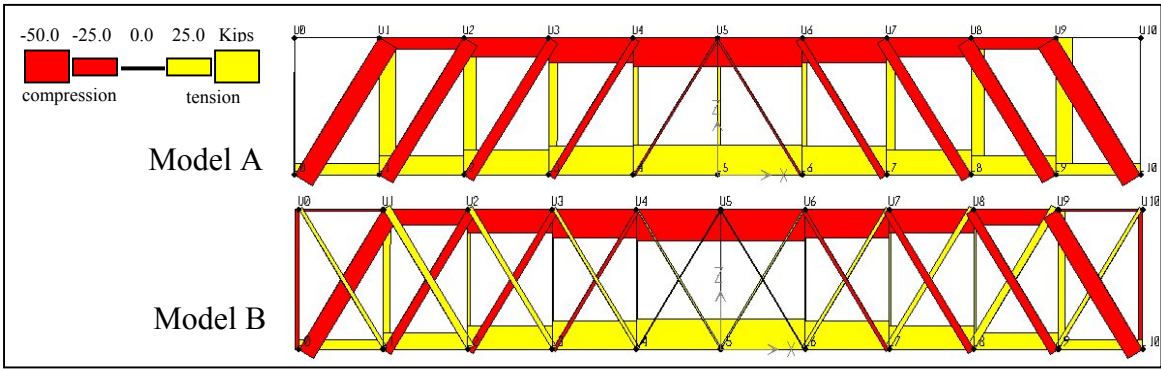


**Fig. 17: Axial forces under dead load in the frame members of the two models.**

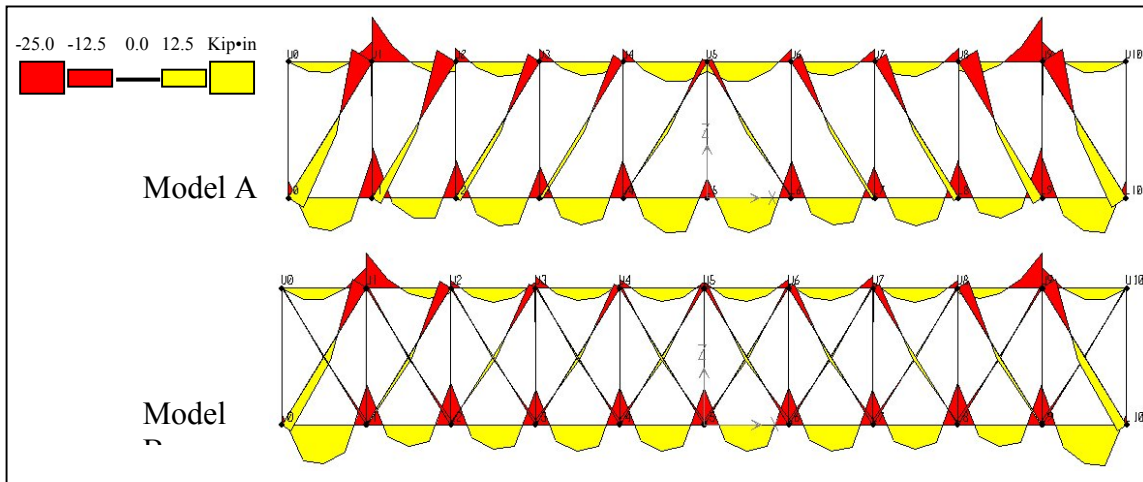


**Fig.18: Bending moments under dead loads in the frame members of the two models.**

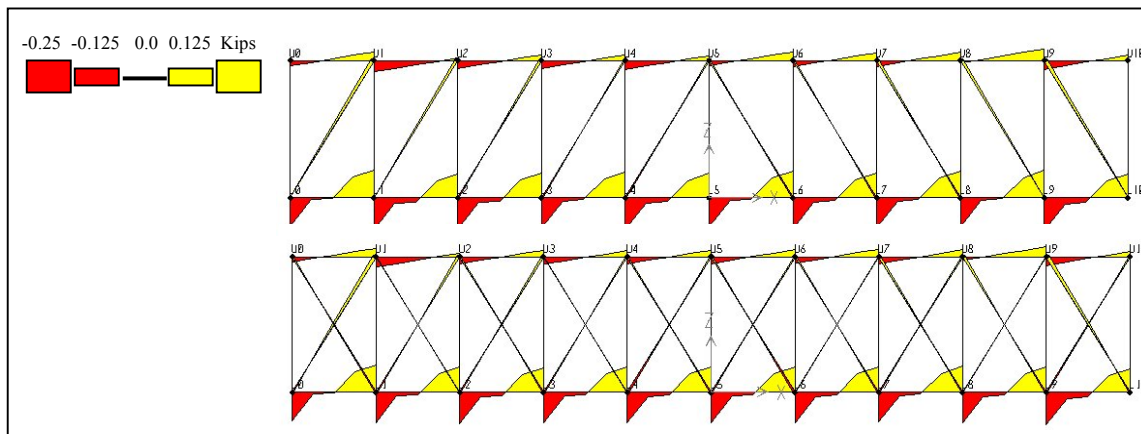


**Fig. 19: Shear forces under dead loads in the frame members of the two models.**

	Element	L4L5 chord	U4U5 chord	L0L1 chord	U0U1 chord	L1U1 post	L0U1 diagonal	L2U1 counter	
	Location	central panel	central panel	final panel	final panel	final panel	final panel	final panel	
Model A	max axial force	kip	42.54	-41.00	15.72	0.0007	23.62	-30.00	--
	max positive bending mom.	kip• in	24.55	14.36	23.63	7.53	0.20	12.45	--
	max negative bending mom.	kip• in	-26.00	-8.88	-29.49	-14.50	-0.24	-16.96	--

	max shear force	kip	-2.29	-0.63	-2.05	0.61	0.00	0.26	--
Model B	max axial force	kip	43.05	-43.57	13.08	-3.11	10.36	-25.05	10.72
	max positive bending mom.	kip•in	18.63	9.70	25.24	7.94	--	7.58	0.85
	max negative bending mom.	kip•in	-26.23	-6.07	-26.45	-14.28	-0.10	-11.57	-1.98
	max shear force	kip	-2.19	-0.51	-0.02	0.62	0.00	0.22	-0.05

**Table 3: Summary of the forces due to dead loads in the main elements of the truss models A and B.**

Regarding forces, shear was almost null and its highest value was about twenty times smaller than the highest axial force. Also stresses due to bending moment were an order of magnitude smaller than stresses due to axial forces. Therefore, despite the continuity of the chords, a truss model with perfect-pin connections may be sufficient to study the bridge behavior.

Regarding the differences between the two models, under dead load the magnitude of the axial forces in the horizontal members does not change significantly (about 2 percent). The counterbraces allow a redistribution of the forces in the diagonal and vertical elements, however, causing a reduction in axial force of about 20 percent in the last panel diagonal and 55 percent in the last panel vertical element.

The stiffening effect of the counterbraces on the truss behavior is clearly demonstrated by the lower nodal displacements. The vertical displacement of the mid-span node on the lower chord, which was the highest in the case of symmetric loading like this, decreases from 0.56 inches in Model A to 0.39 inches in Model B. These values of vertical displacement will increase in time due to creep.

### **Analysis of the Pine Bluff Bridge under Live Loads**

A live load analysis was performed by applying a concentrated unit gravity load (1 kip) on each node along the length of the truss for both models A and B. A live load analysis was also performed by applying a set of unit live loads over one-half the span and on the entire span, corresponding to a uniform distributed load of 12.63 lb/ft<sup>2</sup>.

The results of the analyses were scaled to reflect nineteenth century design live loads. Ketchum describes design live loads for bridges at the end of the nineteenth century.<sup>9</sup> He states that his own specifications were the same as those of the American Bridge Co.'s and those of Theodore Cooper. For "ordinary country highway bridges" Ketchum prescribes for the trusses "a load of 80 lb/ft<sup>2</sup> of total floor surface for spans up to 75 feet; and 55 lb/ft<sup>2</sup> for spans of 200 ft and over; proportionately for intermediate spans." Ketchum also describes the specifications of J.A.L. Waddell and shows Waddell's graph (Figure 20) for live loads for different classes of bridges. Class C is for bridges for "light country service." For a 100' span Waddell prescribes a uniform load of 70 lb/ft<sup>2</sup> and also requires "a concentrated load of 10,000 lbs equally distributed upon two pairs of wheels, the axles of which are 8 ft apart, and the central planes of the wheels 6 ft apart."<sup>10</sup>

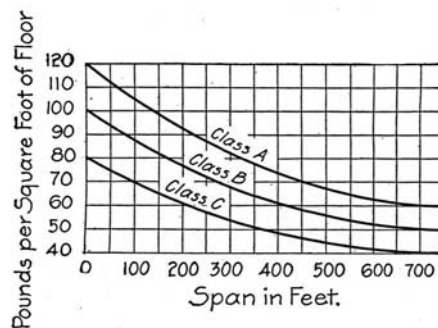


Fig. 22: Waddell's live loads for highway bridges.<sup>11</sup>

Earlier in the nineteenth century, before the existence of model specifications, engineers and builders needed to determine reasonable live loads for their bridge designs. For example, Charles Ellet, in his "Report on the Wheeling and Belmont suspension bridge" (1847), writes: "it is not easy to imagine that a greater load can ever be brought on the flooring of this bridge than that which would be occasioned by covering the carriage-way with as many teams as could stand upon it. A column of sixteen of the six-horse wagons used on the National Road, would occupy the bridge from one abutment to the other." He evaluated the weight per linear foot due to a double line of wagons, fully loaded, and added the weight of 500 hundred persons, obtaining the "greatest transitory load which need be provided against" of 618 lb/ft.<sup>12</sup> He also noted that the total weight of such a load, on his 960' long bridge, would be equal to the weight of 700 head of cattle, or to that of an army of 4,000 men. Dividing the weight per linear foot by the width of the Wheeling Bridge (about 19') reveals that he was designing his bridge for a uniformly

<sup>9</sup> M.S. Ketchum, *The Design of Highway Bridges and the Calculation of Stresses in Bridge Trusses* (New York: The Engineering News Publishing Co., 1909).

<sup>10</sup> J.A.L. Waddell, *The Designing of Ordinary Iron Highway Bridges* (New York: J.Wiley, 1884).

<sup>11</sup> Ketchum, *The Design of Highway Bridges*.

<sup>12</sup> C. Ellet Jr., *Report on the Wheeling and Belmont Suspension Bridge, to the City Council of Wheeling* (Philadelphia: John C. Clark Printer, 1847).

distributed live load of about 32.5 lb/ft<sup>2</sup>. Ellet's live load values have been used for structural analyses of historic bridges.<sup>13</sup>

Each live load analysis also included the full dead load applied simultaneously. The superposition of various loading conditions is allowed since the analyses were carried out with the hypothesis of linear elastic behavior of the bridge. In this case the results of the live load analysis can be scaled for other values of live load and the behavior remains the same.

The live load axial forces in the truss members are plotted in Figures 21 and 22 for the load applied at panel points L2 and L5. Figure 23 shows element forces for a uniform load applied on the first half span of the bridge. The scale at which the forces are plotted is ten times higher than that used in section 5.3 for dead load analysis. The member forces produced by applying only unit live loads are, in fact, an order of magnitude smaller than those produced by the action of dead load alone.

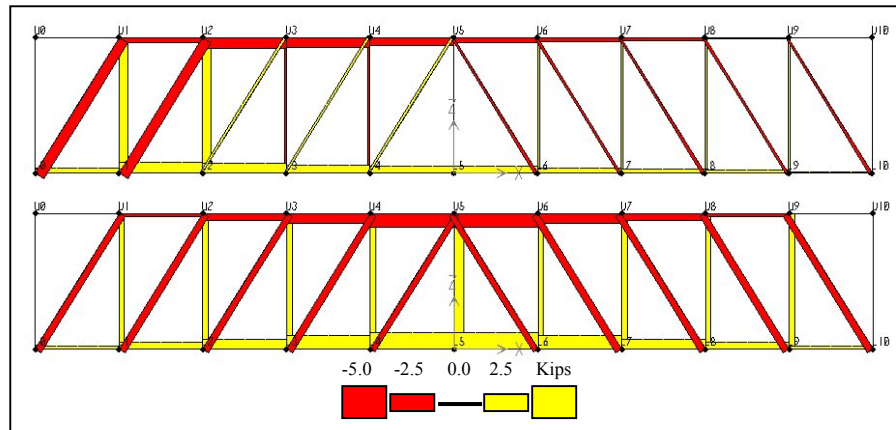
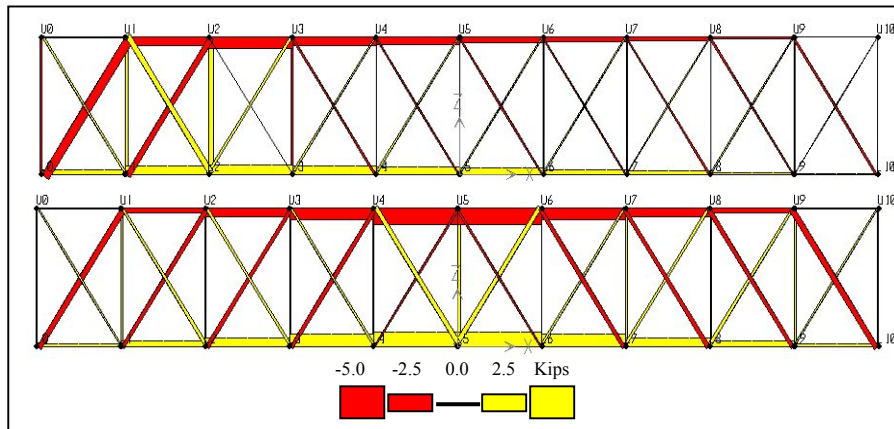
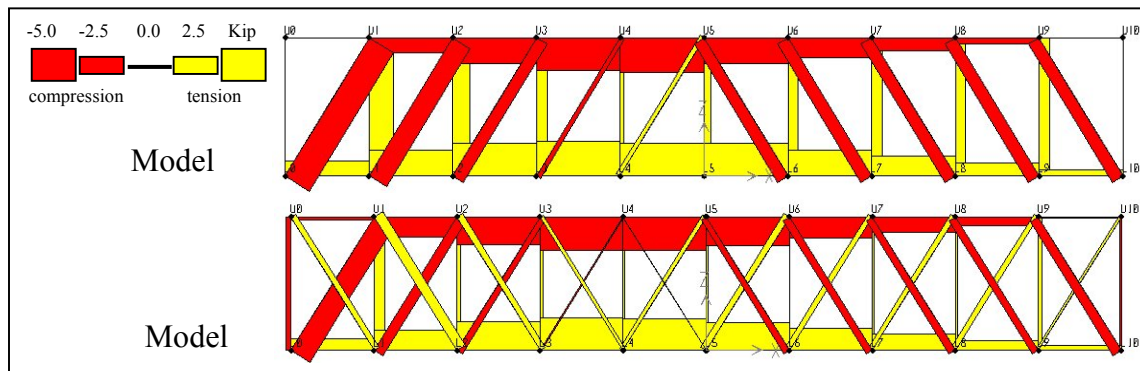


Fig. 21: Model A: axial forces under live loads applied at L2 and L5.

<sup>13</sup> E.L. Kemp and J. Hall, "Case Study of Burr Truss Covered Bridge," *ASCE Engineering Issues—Journal of Professional Activities* 101, no. E13 (July 1975): 391-412.



**Fig. 22: Model B: axial forces under live loads applied at L2 and L5.**



**Fig. 23: Model A and Model B: forces under a uniformly distributed live load over one-half of span.**

In the analysis with uniformly distributed load on the entire span, it was obvious that the central elements of the upper chords were the most axially loaded. An axial force of -7.38 kips and a bending moment of 3.39 kip-in were found in elements U5U6 and U6U7. Scaling these forces for a reasonable value of uniformly distributed live load (40 lb/ft<sup>2</sup> was chosen), the central elements were subject to a compressive stress of -148 psi. The corresponding value of compressive stress due to dead load was -246 psi (axial force and bending moment in the central elements of the upper chord are reported in Table 3, while section areas and moduli of the elements are listed in Table 1. Thus, for reasonable values of live load, the stresses due to dead and live load were of the same order of magnitude. The total compressive stress found, -394 psi, was considerably lower than the maximum allowable stress found in the National Design Specification for Wood Construction.

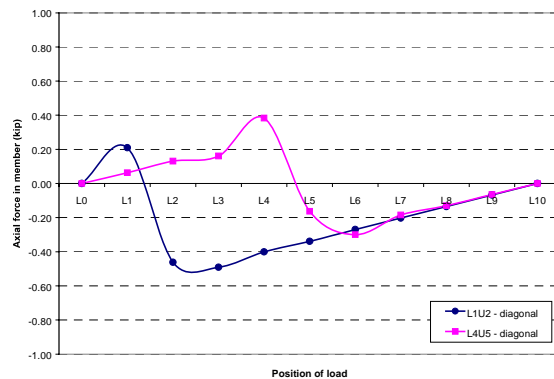
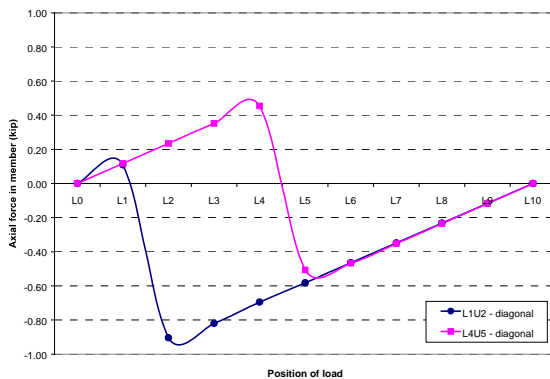
Figure 22 shows that the live load at L2 produces tensile forces in both main diagonals and counterbraces. A uniformly distributed load over a half-span also produces tensile forces in main diagonals and counterbraces, as can be seen in Figure 23. Therefore, to

prevent diagonals from becoming loose, the combined action of dead load and prestressing (tightening of vertical rods) must produce compressive forces that exceed the tensile forces produced by design live loads.

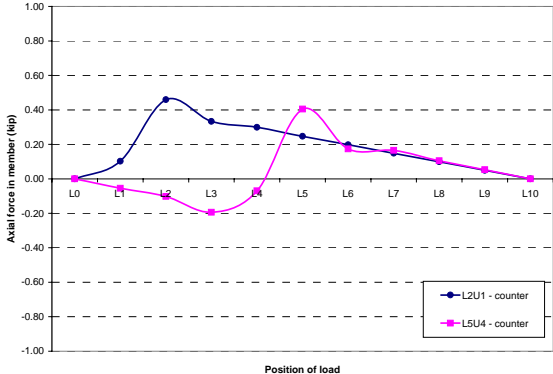
The behavior of the diagonal members for a live load applied at any point on the bridge is also shown through influence lines, which plot the response-force of a particular member versus the location of the live load. The net axial forces due to live load application were considered. Influence lines for unit live load are plotted for elements L1U2 and L4U5 (Figure 24), and for counters L2U1 and L5U4 (Figure 25).

Figure 24 shows that a live load can cause both tensile and compressive forces in the main diagonals. Forces in the diagonal elements of Model B were lower than those of Model A, because of the presence of the counters. Figure 25 shows that a live load causes mainly tensile forces in the counterbraces.

Figure 26 shows the vertical displacements of two panel points on the lower chord (L2 and mid-span point) for different live loads positions. When the live load was moving from the first panel point to a particular node, the node displacement increases more or less linearly. Correspondingly, when the load was moving away from the node, a nearly linear decrease of displacement occurs, except for node L2. Figure 26 also clearly shows that the displacements obtained with counterbraces (Model B), were lower than those without counterbraces (Model A).



**Fig. 24: Model A (left), Model B (right): influence lines of three diagonal members, showing the axial force under a unit live load as a function of load position.**



**Fig. 25: Influence lines of two counters, showing the axial force under a unit live load as a function of load position.**

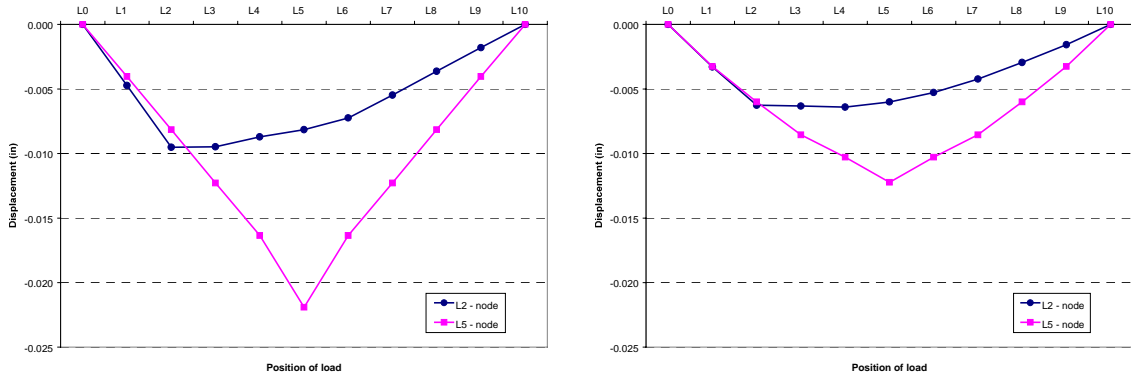


**Fig. 26: Models A (left) and B (right): influence lines of three nodes of the lower chord, showing the displacements under a unit live load as a function of load position.**

The influence lines for the main diagonal members show that the element subjected to the highest axial tension force for the action of a live load application was L4U5, that is to say the mid-span diagonal, when load was applied at node L4. Since the central diagonals are the members subjected to the lowest axial compression due to dead load, they are the members at greatest risk of a zero net axial force due to combined dead and live loads at L4, with the corresponding loosening of diagonal L4U5. Due to the symmetry of the structure, this also applies for diagonal L6U5 when a live load is applied in L6.

Recall that the axial force due to dead load in diagonal L4U5 was equal to -2.92 kip (compression), and that a live load of 1 kip at L4 produces an axial force in the member

of 0.45 kip (tension). Proportionally, the live load equal to 6.49 kip at L4 (equivalent to a total of 6.5 tons for both trusses) will produce a tensile force of 2.92 kip in diagonal L4U5, resulting in a zero net axial force.

The uniformly distributed load that can loosen diagonal L4U5 may be similarly calculated. A set of five live loads of 1 kip applied at panel points L1 to L5 produce an axial force in L4U5 of 0.65 Kip (tension). The set of live loads capable of producing a tensile force of 2.92 kip in the diagonal member is equal to 4.49 kip applied to each panel point on the half span. This is equivalent to a uniform load of about 57 lb/ft<sup>2</sup> on one-half of the bridge.

Under such a concentrated (6.49 tons on the bridge) or uniformly distributed (57 lb/ft<sup>2</sup> on the half span) live load, the structure would become a kinematic mechanism, assuming the hypothesis of perfect pin connections between the truss elements. In reality, the joints of a bridge are not perfect pins. For example, the lower and upper chords are continuous. Because of this continuity of the chords, the bridge does not actually become a mechanism under live loading, but it is clear that this value represents a “critical load” for the structural behavior of the bridge. To prevent loose elements, the diagonals can be prestressed in compression by tightening the vertical rods to put them in tension.

Note that the minimum uniformly distributed live load capable of causing slackness in the diagonals is lower than the design live loads given in late nineteenth century model specifications. On the other hand, the minimum uniformly distributed live load that causes slackness is definitely higher than that used by Ellet in 1847.

### **Prestressing Analyses of the Pine Bluff Bridge**

In Howe’s trusses, tightening the corresponding nuts pretensioned the vertical rods. Model B was used to analyze the effects. The analyses were initially performed by applying unit nodal loads (1 kip) to the frame structure. Different analyses were carried out by first considering each panel prestressed by itself, then all panels prestressed concurrently. The prestressing action of tightening the nuts was modeled by applying additional loads at the nodes and in the directions of the elements being shortened, assuming all nodes were fixed. For example, if vertical element L3U3 is being prestressed the effective nodal loads are as shown in Figure 27.

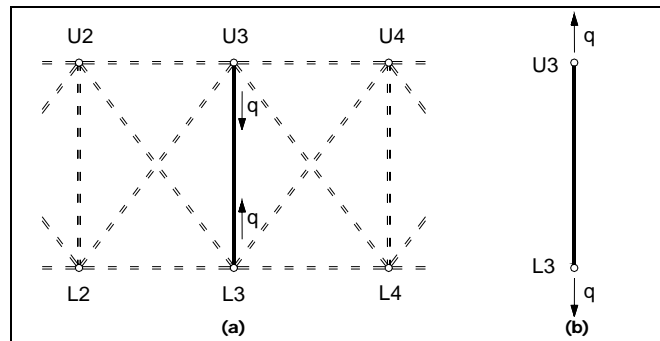


**Fig. 27: Effective nodal loads from tightening a vertical rod (a); corresponding fixed end forces on the rod (b).**

To determine the actual axial force in a rod ( $n_i$ ), the fixed-end force ( $q$ ) must be superposed with the force ( $\mu_i$ ) in the element from the nodal displacement caused by the effective nodal loads, as follows:

$$n_i = \mu_i + q$$

Figure 28 shows axial forces in a portion of the model centered on the vertical rod L3U3, due to effective nodal load from tightening the rod. The rod, L3U3 in this example, was subjected to an axial compressive force of -0.62 kip due to the effective nodal loads and to a fixed end tensile force of 1 kip, for a total actual axial tensile force of 0.38 kip. The two adjoining diagonals and counterbraces were precompressed with an axial force more or less equal in absolute value to half of the axial force acting in the vertical rod (about -0.21 kip). Conversely, the other rods of the two adjacent panels (in average 0.125 kip) and the chords (0.11 kip) were in tension. The distribution of axial forces in the different elements obtained by tightening the rods is a function of the panel's geometry.

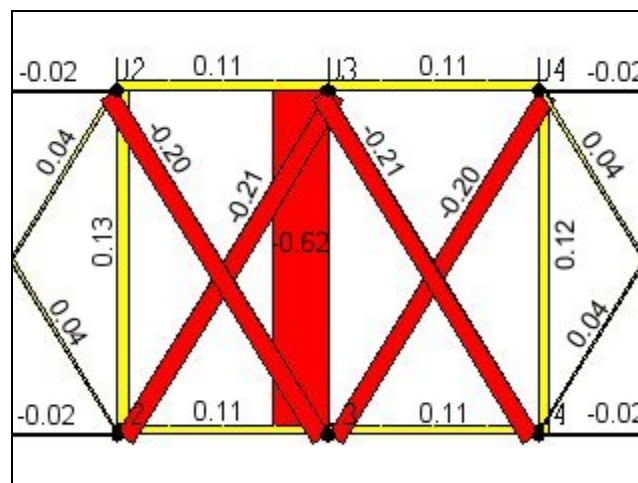


**Fig. 28: Axial forces (kips) from effective nodal loads by prestressing element U3L3. The total force in element U3L3 is found by adding the fixed end force, +1 kip.**

The effect of prestressing on the other panels rapidly decreases to zero. In the two panels that are just beyond those adjoining the tightened rod, the magnitudes of axial forces are an order of magnitude smaller. Thus, the prestressing action obtained by tightening a rod is effective only on the adjoining panels. To achieve the advantages of prestressing in the whole truss, all the rods have to be prestressed.

Figure 29 shows the axial forces from effective nodal loads from prestressing all the vertical elements. The actual axial forces in the rods were found by superposing the fixed end forces to the axial forces produced by the effective nodal loads. It is uncertain how the end rods were tightened, so it was assumed that rods L0U0 and L10U10 were prestressed with the same force used for the other vertical elements.

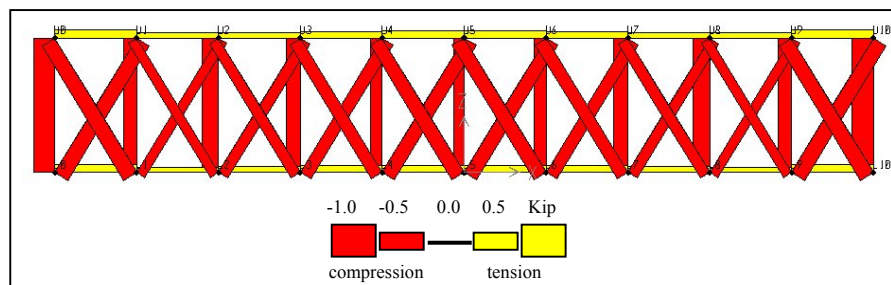


**Fig. 29: Axial forces from effective nodal loads from prestressing all the counters. The total force in the verticals is found by adding their fixed end force, +1 kip.**

The distribution of forces due to prestressing is more or less the same in all of the truss panels. Therefore, the effect of the prestressing with the simultaneous action of a live load should be analyzed in particular for the following truss elements:

- the lower chord element and vertical element subject to the greatest tension, where the prestressing causes an increase of tension
- the main diagonal subject to the greatest compression, where the pretension of the rod produces an increase in compressive force.
- the most highly stressed counter, to see if the effect of precompression is enough to avoid a null net axial force with the consequent loosening of the counter.

The sequence of displacements for nodes L2 and L5, with the application of the prestress nodal loads, is shown in Figure 30. The prestressing sequence chosen started simultaneously from the extremities of the span and proceeded towards the center. At mid-span a more or less linear increase of upward displacement was produced by the sequence of rod tightening. For L2, after a linear increase of upward displacements, the pretensioning of rod L3U3 caused a downward displacement. The last points in the two diagrams represent the total upward displacements of nodes L2 and L5 (mid-span)

produced by prestressing the entire truss. Their values were respectively 0.0007 inches and 0.0018 inches.

The analysis was performed on five different models. In each model only the counterbraces in the panels adjoining the prestressed rods were taken into account. The other counterbraces, as shown in Figure 31, are inactive and do not contribute to the behavior of the truss. Figure 31 shows the model used to evaluate lower chord displacements at the third step of the prestressing sequence, when rods L0U0, L1U1, and L2U2 are pretensioned, and only the counterbraces L1U0, L2U1, and L3U2 (and the correspondent rods and counterbraces on the other half-span) are active.

For the 1 kip effective load, the displacements are very small relative to the predicted dead load displacements. Because of this, if the rods are tightened with falsework in place, the prestressing action will only slightly relieve some of the dead load forces on the falsework. Also, because dead load produces tensile forces in the counters, a truss should be prestressed after the falsework has been removed and the dead load is being carried by the truss alone, although the nut tightening may require more effort.

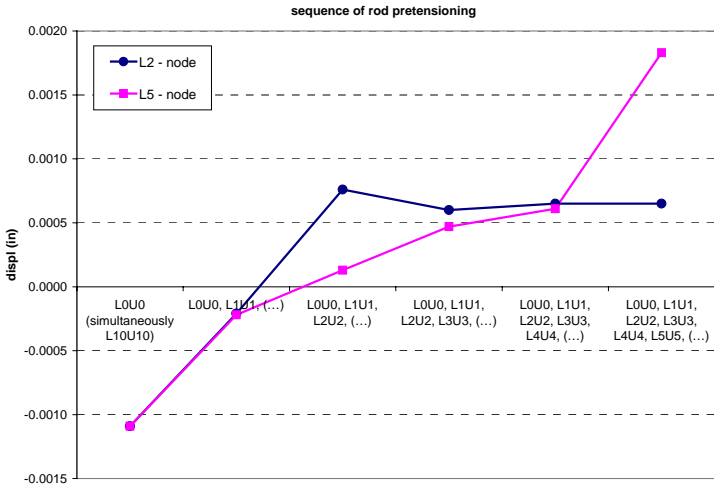


**Fig. 30: Nodal displacement of the lower chord, with the progression of tightening rods.**

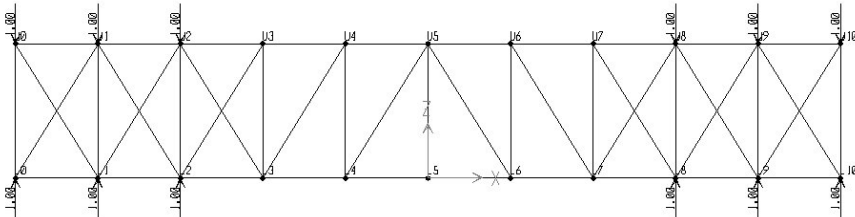


**Fig. 31: Model used to evaluate lower chord displacements at the third step of the prestressing sequence.**

**Analyses Under Dead and Live Loads, With the Effect of Prestressing**

During the experimental studies the actual axial forces produced by tightening a single rod in each of the vertical elements L5U5 and L6U6 were recorded. They were respectively equal to 7.064 kip and 6.635 kip, or 14.128 kip and 13.270 kip on the entire, two-rod vertical elements. These actual prestressing forces ( $N_i$ ) in the rods were used to evaluate the actual prestressing nodal loads applied to the truss. Considering the linear relation between nodal loads and member forces and using the results already found in the case of unit prestress loading the actual prestressing nodal loads ( $Q$ ) were calculated as follows:

$$Q = \frac{N_i}{(\mu_i + q)}$$

The effective nodal loads applied to the truss by rods L5U5 and L6U6 were 28.074 kip and 32.484 kip, respectively. For the analysis of the whole truss, an average value of nodal prestressing loads equal to 30.28 kip was used. The results of the analyses under unit prestress loading and the evaluation of the actual nodal loads are tabulated in Table 4. Table 5 shows axial forces in the vertical elements from the actual prestress loading.

Vertical rod	Axial force due to unit nodal loads $\mu_i$ (kip)	Fixed end force $q$ (kip)	Actual axial force $n_i$ (kip)	Experimental axial force $N_i$ (kip)	Effective nodal loads $Q_i$ (kip)
L0U0 - L10U10		1		--	--
L1U1 - L9U9	-0.728	1	0.272	--	--
L2U2 - L8U8	-0.667	1	0.333	--	--
L3U3 - L7U7	-0.623	1	0.377	--	--
L4U4 - L6U6	-0.591	1	0.409	13.270	32.484
L5U5	-0.497	1	0.503	14.128	28.074

**Table 4: Axial forces in the counterbrace due to a unit prestress loading and effective nodal loads evaluated from the experimental axial forces.**

Vertical rod	Axial force due to effective nodal loads (kip)	Fixed-end force (kip)	Actual axial force (kip)
L0U0 - L10U10	-18.871	30.279	11.408
L1U1 - L9U9	-11.926	30.279	18.353
L2U2 - L8U8	-14.678	30.279	15.601
L3U3 - L7U7	-12.521	30.279	17.758

L4U4 -L6U6	-10.225	30.279	20.054
L5U5	-9.077	30.279	21.202

**Table 5: Axial forces in the counterbraces due to the effective prestress loading.**

Table 6 shows forces for the case of only dead load and for the case of simultaneous dead and prestressing loads. The prestress loading caused a decrease of the axial compressive force due to dead load in the upper chord and an increase of tensile axial force in the lower chord. Both effects varied in intensity with position.

The prestress loading also caused an increase in compression in the diagonals and tension in the vertical rods. This increase was highest in the central panel, where the initial values of axial force were the lowest. The effect of prestressing, therefore, was that of homogenizing the different values of axial forces through the truss. Finally, the counterbraces were subjected to a compressive axial force varying from -12.37 kip (L5U4) to -8.45 kip (L2U1). The upward displacement due to the prestressing was equal to 0.055 inches for the lower chord at mid-span and represents a decrease of about 10 percent of the mid-span displacement under dead load only (0.56 in).

Element	L4L5 chord	U4U 5 chord	L5U5 rod	L4U5 diag.	L5U4 count	L0L1 chord	U0U1 chord	L1U1 rod	L0U1 diag.	L2U1 count
Location	central panel					end panel				
Axial force under dead load kip	42.54	-41.00	3.86	-2.92	--	15.72	.0007	23.62	-30.00	--
Axial force under prestress kip	6.52	6.48	21.20	-12.46	-12.37	6.98	6.95	18.35	-13.36	-8.45
Dead load and prestress kip	49.06	-34.52	25.06	-15.38	-12.37	22.70	6.95	41.97	-43.36	-8.45

**Table 6: Axial forces under dead load and prestress load.**

The analysis of the truss under the simultaneous actions of dead, live, and prestressing loads was used to evaluate the magnitude of live load that could loosen the prestressed counters. With no live load on the truss, the counters with the lowest value of

compressive axial force from prestressing are L2U1 and the symmetric one, L8U9. They have an axial force equal to -8.45 kip under prestressing. L2U1 also has the highest tensile axial force (0.46 kip) when a unit live load (1 kip) is applied at L2. Therefore, the greatest risk for combined prestressing and live loads to produce a zero net axial force state in one of the counterbraces corresponds to the application of a live load at L2, with the corresponding loosening of counter L2U1. Due to the symmetry of the structure, all the previous and following considerations can be repeated for the corresponding counter L8U9 when a live load was applied in L8. Assuming linearity and using superposition, the minimum live load capable of loosening these counterbraces can be calculated. A live load of 18.37 kip applied on truss node L2 can loosen counterbrace L2U1.

Using the same procedure, the uniformly distributed load needed to loosen counterbrace L2U1 was calculated. When a set of five unit live loads was applied at panel points L1 to L5, a tensile axial force of 1.44 kip was produced in L2U1. By proportion, the set of live loads capable of producing a tensile force of -8.45 kip in the diagonal member, i.e. a zero net axial force in the diagonal, was equal to 5.87 kip applied to each panel point on half span, equivalent to a uniform load of about 74 lb/ft<sup>2</sup> on half of the bridge. Therefore, the minimum concentrated live load capable of loosening a counterbrace corresponds to a live load of about 18 tons on the bridge, which is more than three times the current load limit. The minimum distributed live load required to loosen a counter was equal to 74 lb/ft<sup>2</sup>. This value is 128 percent higher than the design live load used by Ellet in 1847. The values of minimum concentrated load and uniform load that causes slackness are, respectively, 260 percent and 6 percent higher than those specified by Waddell. As long as the compression force in the counters from prestressing is not reduced to zero by a live load, the counters will remain effective in helping to carry live load and stiffen the bridge.

### **Effects of Shrinkage and Creep on Bridge Behavior**

Shrinkage and creep are deformations related, respectively, to changes in moisture content and the behavior of wood under load. Both shrinkage and creep are time-dependent phenomena. Shrinkage involves a reduction in dimensions of the truss members as the wood loses moisture and, thus, volume. It is a normal and typical process in the wooden elements used to build bridges, especially those built using wood that was still green.

In reality, if a wooden element is restrained, its shrinkage will be hindered and the restraints will induce a tensile stress on the element. Therefore, the corresponding behavior of the truss under shrinkage can be evaluated by computing the forces in the truss elements when all the shrinkage nodal loads are applied, and then superposing the effect of the fixed-end forces, as done in the prestress analyses. The behavior of the truss under creep can be evaluated in the same way already mentioned for shrinkage, taking into account the actual state of stress of the elements before creep starts.

Both creep and longitudinal shrinkage cause displacements and, possibly, decreases in prestressing forces in the counterbraces. Therefore, some analyses of the truss under the combined actions of shrinkage and creep were carried out using Model B to evaluate their influence on the initial, prestressed state. Unlike wood, iron does not shrink or creep, so these considerations apply only to the wooden elements.

For the shrinkage analysis, a value of strain equal to 0.002 was used. This is equal to the longitudinal shrinkage, from green to oven dry, for a large number of wood species. This value could be reduced to take into account the fact that the actual shrinkage of the bridge elements is from a green moisture content of 30 percent to something in the range of 12 to 19 percent, depending on a variety of circumstances. However, considering that the tangential and radial shrinkage at the nodes was not modeled, the conservative value of 0.002 was used.

The effective nodal loads ( $S_i$ ) due to longitudinal shrinkage were calculated for each element as follows, where  $\varepsilon_s$  is the shrinkage strain,  $E$  the modulus of elasticity of wood, and  $A_i$  the area of the  $i$ -element:

$$S_i = \varepsilon_s \cdot E \cdot A_i$$

The results of the shrinkage analyses are listed in Table 7. The actual axial forces from shrinkage are almost null in all the elements. This is because the entire structure is free to shrink and the shrinkage is uniformly distributed in all the elements. A shrinkage analysis performed on Model A also produced essentially no axial forces.

Assuming a large value of longitudinal shrinkage to take into account the effect of tangential and radial shrinkage can be a conservative hypothesis. In the case where the cast-iron bearing shoes were properly made, that is to say that they have flanges against which the nuts are tightened, there would be no bearing on the horizontal elements and their shrinkage should not affect the connections with the main and counter diagonals at all. If the bearing shoes have no flanges, as in the Pine Bluff Bridge, there will be an effect of bearing on the upper and lower chords and therefore the effect of tangential and radial shrinkage should produce a decrease of prestressing in the diagonals.

For the creep analyses, two different procedures for the evaluation of creep nodal loading were used. One uses empirical data from the National Design Specification for Wood Construction, while the other employs a theoretical European method.

Element		Geometry		Dead load and prestressing		Shrinkage		
Name	Type	Length (in)	Area (in <sup>2</sup> )	Axial force prest. (kip)	Axial force dead & p. (kip)	Fixed end axial force (kip)	Axial force from nodal loading (kip)	Actual axial force (kip)
L0L1	lower chord	120	232.9	6.97	22.70	558.96	-585.40	-26.44
L0U0	vertical rod	195	1.57	11.41	10.99	--	-42.90	-42.90
L0U1	diagonal	229	144	-13.36	-43.15	345.6	-294.80	50.80
L1L2	lower chord	120	232.9	4.43	31.91	558.96	-589.35	-30.39
L1U0	counter	229	36	-13.25	-13.25	86.4	-36.15	50.25
L1U1	vertical rod	195	3.53	18.35	41.86	--	-92.89	-92.89
L1U2	diagonal	229	128	-8.42	-30.70	307.2	-249.09	58.11
L2L3	lower chord	120	232.9	5.08	41.01	558.96	-584.97	-26.01
L2U1	counter	229	48	-8.45	-8.45	115.2	-57.22	57.98
L2U2	vertical rod	195	3.08	15.60	33.45	--	-91.67	-91.67
L2U3	diagonal	229	112	-9.75	-25.76	268.8	-219.02	49.78
L3L4	lower chord	120	232.9	5.84	46.84	558.96	-583.69	-24.73
L3U2	counter	229	48	-9.69	-9.69	115.2	-65.64	49.56
L3U3	vertical rod	195	2.53	17.76	30.12	--	-82.57	-82.57
L3U4	diagonal	229	112	-11.16	-20.77	268.8	-221.56	47.24
L4L5	lower chord	120	232.9	6.52	49.06	558.96	-579.11	-20.15
L4U3	counter	229	56	-11.15	-11.15	134.4	-87.25	47.15

L4U4	vertical rod	195	1.99	20.05	26.91	--	-73.03	-73.03
L4U5	diagonal	229	96	-12.46	-15.38	230.4	-191.95	38.45
L5U4	counter	229	64	-12.37	-12.37	153.6	-115.28	38.32
L5U5	vertical rod	195	1.57	21.20	25.06	--	-65.15	-65.15
U0U1	upper chord	120	202.5	6.95	6.95	486	-512.34	-26.34
U1U2	upper chord	120	202.5	4.40	-11.32	486	-516.29	-30.29
U2U3	upper chord	120	202.5	5.08	-22.40	486	-511.97	-25.97
U3U4	upper chord	120	202.5	5.84	-30.09	486	-510.67	-24.67
U4U5	upper chord	120	202.5	6.48	-34.53	486	-506.05	-20.05

**Table 7: Fixed-end forces, axial forces from nodal displacements and effective axial forces from shrinkage in Model B.**

In the first, a value of strain equal to the initial elastic strain was used. The National Design Specification for Wood Construction (NDS) suggests this value for the case of green wood in bending, and it has been confirmed by some empirical research.<sup>14</sup> Most of the data used to evaluate a creep factor for the analysis of the Pine Bluff Bridge was extrapolated from this research on creep in bending, instead of creep for axial loading, and on wood species different from white pine. The rationale for believing this data to be applicable is that, under steady moisture, creep deformation at a given percentage of the ultimate strength is roughly equal in compression, bending, and tension parallel to the grain, and that there is no marked difference in the creep behavior of wood among the different species.<sup>15</sup> For the second analysis, the creep strain was calculated using the equation given by the Eurocode 5.<sup>16</sup>

The effective nodal loads from creep ( $C_i$ ) using the first procedure, were calculated for each element using the following formula:

$$C_i = \varepsilon_e \cdot E \cdot A_i$$

where  $\varepsilon_e$  is the initial elastic strain,  $E$  the modulus of elasticity of wood and  $A_i$  the area of the  $i$ -element. In the second procedure, the effective nodal loads ( $C_i$ ) were computed as follows:

$$C_i = \left\{ \frac{\sigma_i}{E} \cdot [1 + 0.30(1 + 0.30(1 - e^{-t}))] \right\} \cdot E \cdot A_i$$

where  $\sigma_i$  is the applied constant stress in the elements and the time  $t$  (in hours) was taken equal to two years. This period of time factored in was two years, which available literature considers sufficient for creep to stabilize. Actually, this formula assumes a very high rate of creep, such that the values of strain after twenty-four hours were almost the same as those after two years.

After computing the axial forces from nodal displacements, the fixed-end forces were superposed on all the elements, and the actual axial forces due to creep were found. The values of the fixed-end forces, the axial forces from nodal displacements, and the effective axial forces due to creep are tabulated in Table 8.

Comparing the two methods, the creep nodal loads and the corresponding axial forces in the truss elements determined using the NDS empirical rule are 28 percent lower than those calculated by the Eurocode 5 formula. The resulting changes in axial forces from

---

<sup>14</sup> K.J. Fridley, "Designing for Creep in Wood Structures," *Forest Products Journal* 42, no. 3 (1992): 23-28.

<sup>15</sup> R.S.T. Kingston, "Creep, Relaxation and Failure of Wood," *Research Applied in Industry* 15, no. 4 (1962): 164-170.

<sup>16</sup> J. Tissaoui, "Effects of Long-Term Creep on the Integrity of Modern Wood Structures" (Ph.D. diss., Virginia Polytechnic Institute and State University, December 1996).

creep, as calculated from the EC5, were 38 percent higher than those produced by creep as calculated by the NDS.

Element		Geometry		Dead load and prestressing		Creep (NDS)			Creep (EC5)		
Name	Type	Length (in)	Area (in <sup>2</sup> )	Axial force prest. (kip)	Axial force dead & p. (kip)	Fixed end axial force (kip)	Axial force from nodal loading (kip)	Actual axial force (kip)	Fixed end axial force (kip)	Axial force from nodal loading (kip)	Actual axial force (kip)
L0L1	lower chord	120	232.9	6.97	22.70	22.70	17.00	-5.70	31.55	23.62	-7.92
L0U0	vertical rod	195	1.57	11.41	10.99	--	-9.23	-9.23	--	-12.84	-12.84
L0U1	diagonal	229	144	-13.36	-43.15	-43.15	-32.25	10.89	-59.97	-44.84	15.13
L1L2	lower chord	120	232.9	4.43	31.91	31.91	28.47	-3.44	44.36	39.60	-4.76
L1U0	counter	229	36	-13.25	-13.25	-13.25	-2.41	10.83	-18.41	-3.35	15.06
L1U1	vertical rod	195	3.53	18.35	41.86	--	-14.78	-14.78	--	-20.55	-20.55
L1U2	diagonal	229	128	-8.42	-30.70	-30.70	-24.18	6.52	-42.67	-33.61	9.06
L2L3	lower chord	120	232.9	5.08	41.01	41.01	37.41	-3.60	57.01	52.02	-4.99
L2U1	counter	229	48	-8.45	-8.45	-8.45	-1.99	6.46	-11.75	-2.77	8.98
L2U2	vertical rod	195	3.08	15.60	33.45	--	-11.30	-11.30	--	-15.71	-15.71
L2U3	diagonal	229	112	-9.75	-25.76	-25.76	-18.98	6.78	-35.81	-26.38	9.43
L3L4	lower chord	120	232.9	5.84	46.84	46.84	43.98	-2.86	65.11	61.15	-3.96
L3U2	counter	229	48	-9.69	-9.69	-9.69	-2.95	6.74	-13.47	-4.10	9.37
L3U3	vertical rod	195	2.53	17.76	30.12	--	-10.26	-10.26	--	-14.25	-14.25
L3U4	diagonal	229	112	-11.16	-20.77	-20.77	-15.45	5.32	-28.87	-21.48	7.39
L4L5	lower chord	120	232.9	6.52	49.06	49.06	46.93	-2.14	68.20	65.25	-2.95
L4U3	counter	229	56	-11.15	-11.15	-11.15	-5.84	5.31	-15.50	-8.12	7.38
L4U4	vertical rod	195	1.99	20.05	26.91	--	-7.92	-7.92	--	-11.00	-11.00
L4U5	diagonal	229	96	-12.46	-15.38	-15.38	-11.46	3.92	-21.38	-15.93	5.45
L5U4	counter	229	64	-12.37	-12.37	-12.37	-8.39	3.98	-17.19	-11.66	5.53
L5U5	vertical rod	195	1.57	21.20	25.06	--	-6.69	-6.69	--	-9.30	-9.30
U0U1	upper chord	120	202.5	6.95	6.95	6.95	1.27	-5.68	9.65	1.75	-7.90
U1U2	upper chord	120	202.5	4.40	-11.32	-11.32	-14.69	-3.37	-15.73	-20.42	-4.69
U2U3	upper chord	120	202.5	5.08	-22.40	-22.40	-25.89	-3.49	-31.14	-36.01	-4.87
U3U4	upper chord	120	202.5	5.84	-30.09	-30.09	-32.82	-2.72	-41.83	-45.63	-3.80
U4U5	upper chord	120	202.5	6.48	-34.53	-34.53	-36.55	-2.02	-47.99	-50.82	-2.82

**Table 8: Fixed-end forces, axial forces from nodal displacements and effective axial forces from creep.**

Comparing axial forces from creep with axial forces from prestressing, in the case of creep evaluated with the EC5, it is evident that creep can loosen the two prestressed counterbraces closest to the truss ends (L1U0, L2U1), but its effect is not sufficient to completely loosen the counterbraces closest to mid-span (L3U2, L4U3, L5U4). In the case of creep evaluated by the use of NDS, creep is not sufficient to loosen the counterbraces, but it can cause a decrease of compressive axial force in the counterbraces of up to 82 percent (L1U0). The changes in forces due to creep were smaller than those produced by shrinkage, being of the same order of magnitude as the forces from prestressing.

To predict the times at which one or more counterbraces become loose, a model for creep rate as function of stress would be required. A qualitative “rule-of-thumb” for wood in a constant stress condition is that about 25 percent of the total creep occurs within the first day, 50 percent occurs within the first week, and 75 percent occurs within the first month. As a general rule, nuts need to be tightened more often during the early stages in a bridge’s life (within the first year) and less often later. Finally, the downward mid-span displacements due to creep were found to be 0.30 inch and 0.42 inch, respectively, using the NDS and EC5 techniques. Thus, it is evident that creep can cause displacements more or less equal to the initial ones experienced under dead load and prestressing (0.33 in).

### **Experimental Testing on the Pine Bluff Bridge**

Considering the major feature of Howe’s truss, which is the pretensioning of the vertical rods by tightening the nuts, experiments on the Pine Bluff Bridge were carried out with one main aim: evaluating the probable prestressing load that can be achieved in the rods by manually tightening the nuts and measuring the forces produced in the other members of a prestressed panel. The measurement of the prestressing load in the rods was used to define the forces for the prestressing analyses of the bridge.

Furthermore, measurement of the displacements of the bridge under a live load allowed checking the reliability of the model by comparing the actual displacements obtained during the experimental tests to those evaluated by numerical modeling. The discrepancy found between the tests and the models results guided a revision of the model itself and suggested a better definition of the material properties, which can be different from the average values used in the finite element modeling due to damage and aging effects.

### **Description of the Experiments**

The tests carried out on the Pine Bluff Bridge were completed in two days, June 17 - 18, 2002. Two basic kinds of tests were performed. One consisted of measuring the strains in the vertical wrought iron rods and in the wooden members of some panels in the northwest truss, while tightening the nuts of some of the vertical rods. The other

consisted of measuring the displacements of the two bottom chords of the bridge at mid-span, on the north span of the bridge, while driving a truck above the bridge. Table 9 lists the tests performed.

Kind of test	Test repetitions	Instruments	Performed analyses
Prestressing of rod L5U5	three	14 strain trans. 2 Strain gages	Strain-stress in the elements
Prestressing of rod L6U6	once	14 strain trans. 4 strain gages	Strain-stress in the elements
Truck of known weight traversing the bridge	three	14 strain trans. 4 strain gages 2 displ. trans.	Mid-span displacements Strain-stress in the elements

**Table 9: Tests performed on the Pine Bluff Bridge.**

The test equipment consisted of fourteen strain transducers, with a 5-inch gauge length, four electrical resistance strain gages, one inductive displacement transducer (DCDT), and a potentiometer (also used for displacement measurement). A multi-channel data logger (Figure 32) was used for the collection and the analog-digital conversion of the data. This was connected to a laptop computer that recorded the data and checked it for reasonableness. The sample interval was 1 per second in all tests. The data-logger and computer were time-synchronized prior to test initiation.

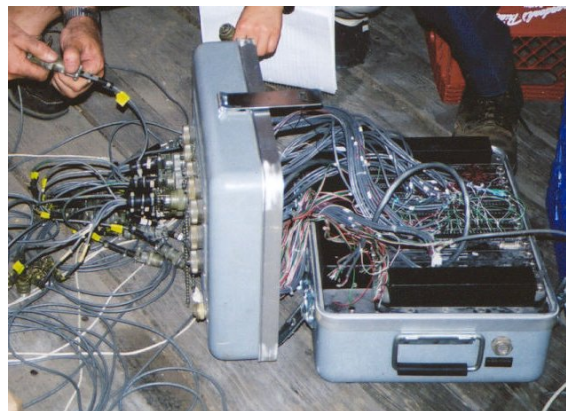


**Fig. 32: Data logger for experimental data acquisition, field photograph.**

Prior to the tests, a condition assessment of the bridge was conducted. The conditions of the counterbraces were checked, in order to verify whether they were tight or slack. Furthermore, a visual inspection of construction details, damage and previous repairs was

made, in order to interpret possible anomalies in the test results. Finally, the decision of performing the prestressing tests on the rods of the northwest truss was made.

During the prestressing test on rods L5U5 and L6U6 (northwest truss), the existing nuts were manually re-tightened with the use of a wrench, attempting to reproduce the original construction technique of the bridge. The strains produced by prestressing the rods were measured with strain gages (Figure 33a), in the counterbrace and the diagonal of panel L5U5-L6U6 and in the diagonals of panels L6U6-L7U7 and L7U7-L8U8, with the use of the fourteen available strain transducers. The counterbrace and both the timbers that compose the main diagonals (Figure 33b) were instrumented with two strain transducers each. These were applied on the extreme fibers of the elements, in order to evaluate the average strain and detect possible bending on the members.



**Fig. 33: Strain gauge on a rod (a) and strain transducers on diagonal elements (b), field photograph.**

Stresses were calculated by multiplying the measured strains by the modulus of elasticity for white pine ( $1.2 \times 10^6$  psi) or wrought iron ( $2.8 \times 10^7$  psi). Also, the total axial forces were calculated by multiplying these unit stresses by the sectional areas of the appropriate members. This gave an indication of the possible prestress forces that can be produced in the various elements of Howe trusses by tightening the nuts on the vertical rods.

Two displacement transducers and a potentiometer were placed under the northern bottom chords, at mid-span (Figure 34).

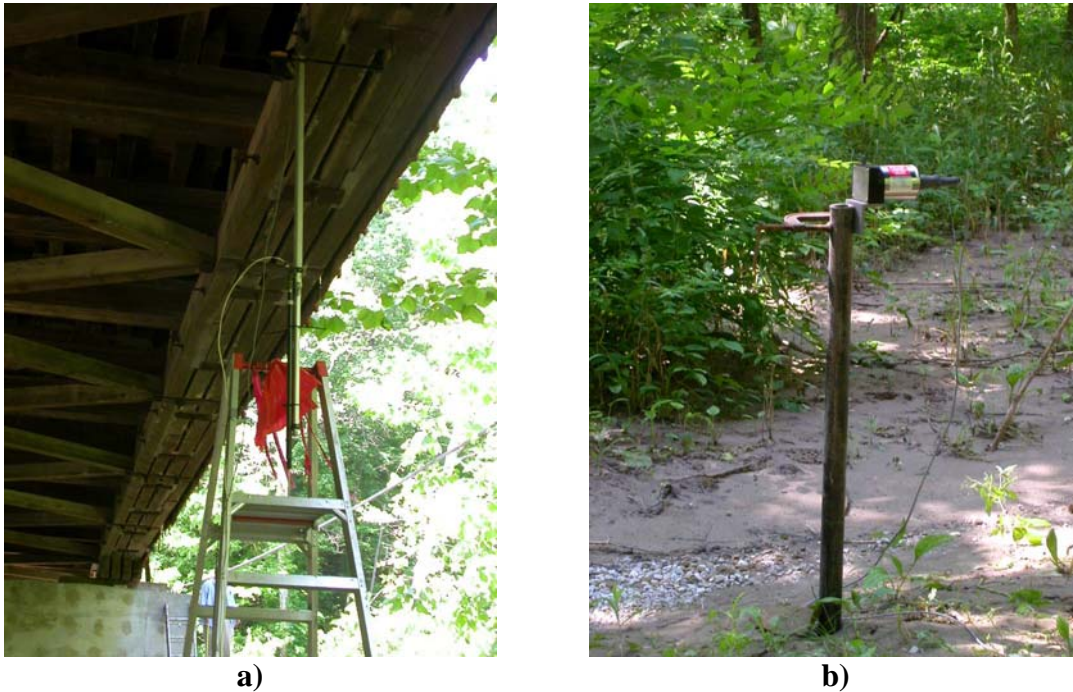


**Fig. 34: Displacement transducer (a) and potentiometer (b) used for displacement measurements, field photographs.**

The live load was applied by driving a truck weighing approximately 6 tons on the bridge (Figure 35). The truck was driven along the center of the deck to avoid uneven distribution of the load between the parallel trusses, and slowly in order to minimize dynamic effects. In each test the truck was moved from north to south, and it was stopped for about 10 seconds, to allow stabilization in the DCDT data acquisition, in five different spots (L8, L6, mid-span [L5], L4, and L2).



**Fig. 35: Live load testing with the 6-ton truck, field photograph.**

### Results of the Prestressing of the Vertical Rods

The different “prestressing tests” on the vertical rods lasted from 2 to 4 minutes. This was the range of time necessary to tighten the previously loosened nuts as much as possible. The test was performed by loosening only one rod of the vertical element at once. Both rods cannot be loosened simultaneously without deforming the truss.

The strains in the rods, measured as averages of the various tests, were equal to 321.3  $\mu$ strain for L5U5 (1-inch diameter) and 238.4  $\mu$ strain for L6U6 (1.125 inch-diameter), which correspond respectively to average tensile stresses of 8,996.4 psi and 6,675.2 psi and average tensile axial forces equal to 7,064 lb and 6,635 lb. Consequently, prestressing forces were also produced in the main diagonals and in the counterbraces of the tested panels. As expected, they were subjected to an axial force of compression.

Figures 36 and 37 show the results of the “prestressing test” performed, in terms of strains and axial forces produced in the rods. Note that tightening a nut on a rod of a vertical element causes a decrease of strain, that is to say a release of stress, in the other, parallel rod. In the same way, when a pretensioned rod was loosened, the other rod recovered its original strain and stress condition.

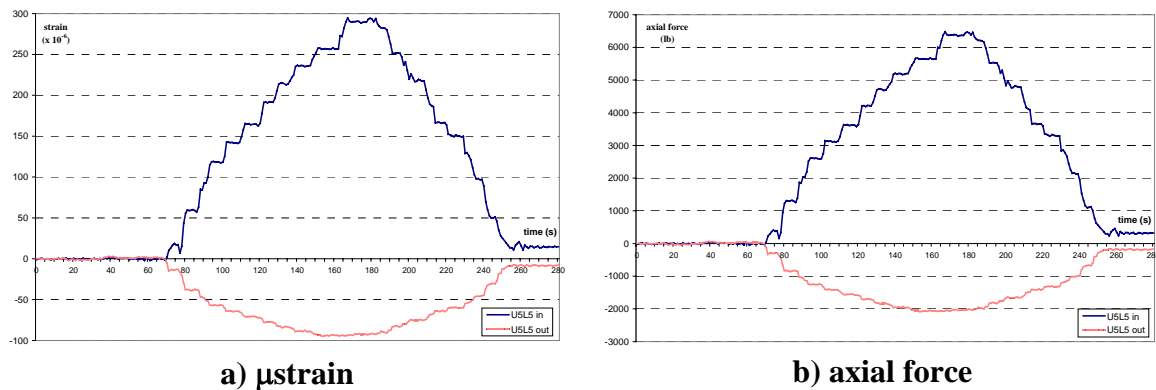


**Fig. 36: Tightening of inside rod of element U5L5: strain (a) and axial forces (b) in the outside and inside rod.**

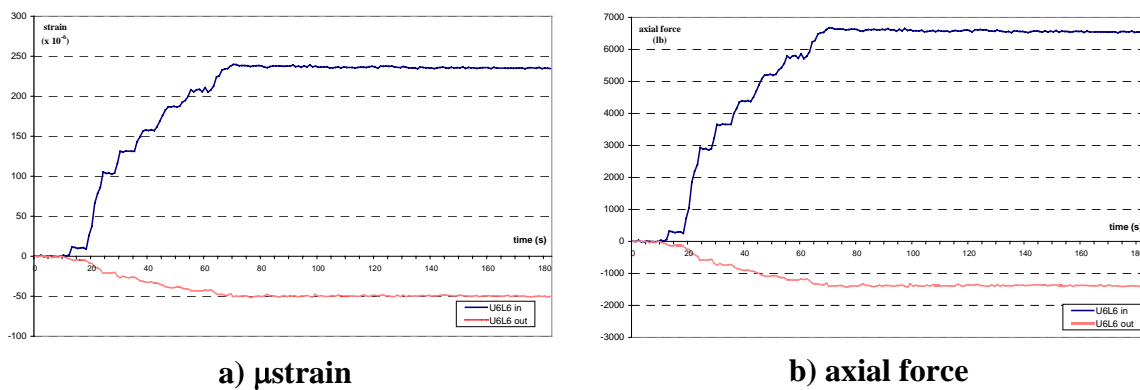


**Fig. 37: Tightening of inside rod of element U6L6: strain (a) and axial forces (b) in the outside and inside rod.**

Figures 38 and 39 show strains and axial forces in the diagonal elements of panel L5U5-L6U6 while tightening the inside rod of L5U5 and the inside rod of L6U6, respectively. It can be clearly seen that the effect of tightening only one of the two rods of a vertical element was felt only by the corresponding main diagonal timber. The strains in the outside timbers of the main diagonals were, in fact, almost null when tightening the inside rods.

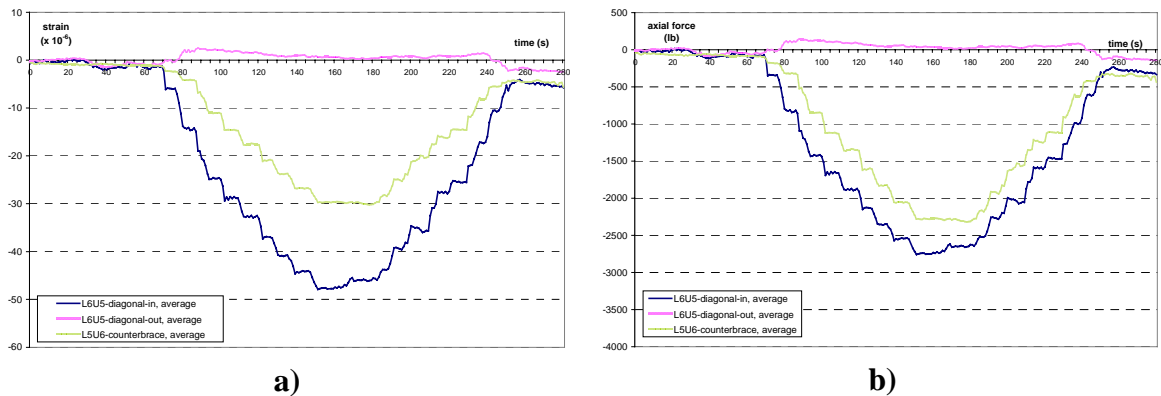


**Fig. 38: Strains (a) and axial forces (b) produced in the diagonal elements of panel L5U5-L6U6 by tightening the inside rod of U5L5.**

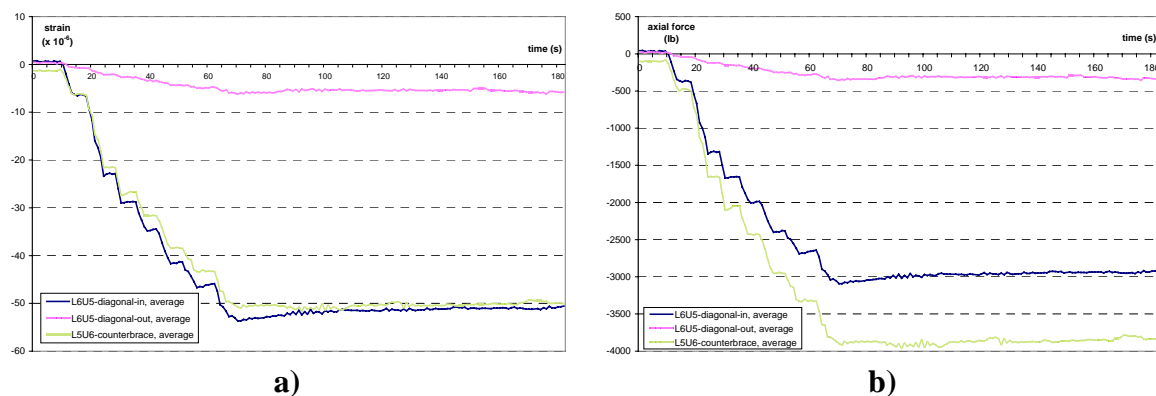


**Fig. 39: Strains (a) and axial forces (b) produced in the diagonal elements of panel L5U5-L6U6 by tightening the inside rod of U6L6.**

### Result of the Live Load Tests

Figures 40 and 41 show the displacements of the bottom chords at mid-spans for various positions of the applied load. The displacements are plotted with reference to time; therefore, the movement of the truck on the bridge deck can be easily recognized in the diagrams. The slopes correspond to increases or decreases of the bottom chord mid-span displacements while the truck was moving on the deck. On the contrary, the horizontal

lines in the diagrams are the displacements when the truck was stopped at various positions (respectively L8, L6, mid-span [L5], L4 and L2). These flat areas of the diagrams correspond to deflections under static loading. During the first test, the truck was shifted towards the east side of the bridge and consequently the displacements of the east chord were higher than those of the west chord. The test was repeated running the truck nearer to the center of the deck, and the maximum differences between the west and east chord displacements changed from 41 percent to only about 19 percent.

The average displacements of the north chord when the live load was applied at mid-span were of about 0.216 inch the three tests performed. In particular, the northeast mid-span displacement was about 17 percent higher than the northwest displacement in the tests with the truck close to the center of the deck. The initial non-zero reading of displacement was subtracted to obtain the actual mid-span displacement values.

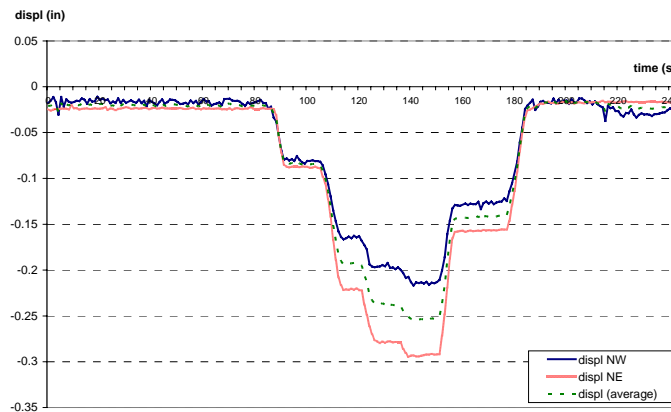


**Fig. 40: Mid-span displacements under live load.**

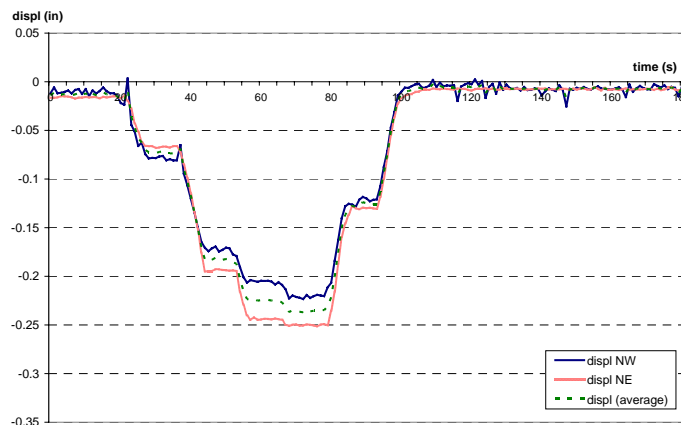


**Fig. 41: Mid-span displacements under live load with the truck close to the center of the deck.**

Interestingly, after the live load was applied at L6 and at L5 (mid-span), a further increase of mid-span displacement was registered when the truck moved to L4. This

could be related to the fact that both vertical elements L6U6 and L5U5 had been previously retightened, while L4U4 was not. The slackness of some of the original vertical rods had been noted during the inspection of the bridge.

Strains in selected members of the northern span were also measured. Axial forces were computed by multiplying the strains by the modulus of elasticity of the wood ( $1.2 \times 10^6$  psi) and the section area. Figure 42a shows that, after re-tightening the nuts, both the counterbrace and the main diagonal were active in carrying the live load.

A maximum positive  $\mu$ strain equal to 39  $\mu$ strain, which corresponds to an axial tensile force of 2,995 lb, was measured in the counterbrace. For the main diagonal timbers the maximum negative strains were equal to -16.3  $\mu$ strain and -7.8  $\mu$ strain, which correspond to axial compressive forces of -938.9 lb and -449.3 lb, respectively (Figure 42a). These strain measurements reflect the effect of the live load only, because all the instruments were reset after re-tightening the vertical rods.

The strains produced in the diagonal elements by tightening the rods L5U5 and L6U6 had been previously measured during the “prestressing test”. In the last prestressing test before the live load test they were equal in average to -104, -34.5 and -112  $\mu$ strain, respectively in the inside and outside timber of the main diagonal L6U5 and in the counterbrace L5U6. These strains were added to those due to the action of live load in Figure 42b in order to make a qualitative evaluation of the strain in the wooden members with the simultaneous action of prestressing and live load.

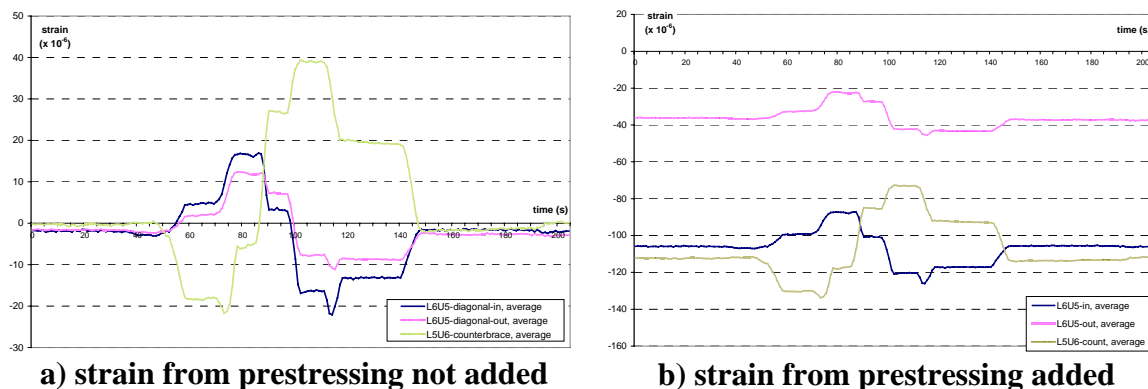


**Fig. 42: Average strains in the diagonal elements of panel L5U5-L6U6 under live load, with strains produced by prestressing not added (a) and added (b).**

As can be seen, the negative strain in the main diagonal increased to a maximum average negative value of -81  $\mu$ strain, which corresponds to an axial compressive force of -4,666 lb, when the live load was applied at L4. For the same load position, the strain in the counterbrace decreased from the negative value of -112  $\mu$ strain produced by the precompression, to a negative value of -73  $\mu$ strain, which corresponds to an axial force of -5,606 lb. Therefore, during the live load application, the counterbrace does not reach a

zero axial force state, but remains in compression. Thanks to the prestressing action, the counter does not separate from the structure, contributing to the stiffness of the bridge.

Figure 43 shows the evolution of average strain in the various elements instrumented with strain transducers, as the live load traversed the bridge. In this diagram the previous strains due to the prestressing have not been considered. The necessity of proper prestressing to keep the counterbraces active in compression under live loads, is again clear.

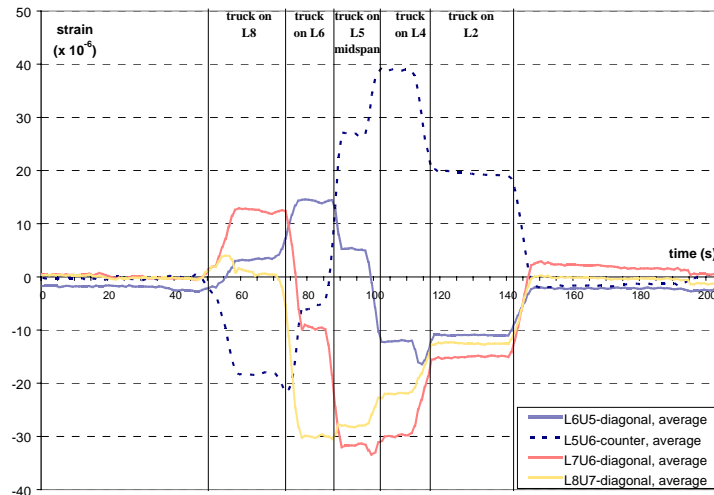


**Fig. 43: Average strains in the diagonal elements of the truss under live load, (strains from prestressing are not added).**

### Comparison Between Experimental Testing and Numerical Modeling

The first comparison between the experimental measurements and the numerical results of the structural analyses was made for the mid-span displacements. When a 6 kip load was applied at the north mid-span, the average mid-span displacement experimentally measured was equal to 0.216 inch. The result of the structural analyses using Model A was equal to 0.131 inch, a difference of -39 percent.

The reduced stiffness of the actual bridge compared to the numerical model could have several causes. Aging and/or decayed wood, with a consequent reduction of elastic properties and sections, is a possibility. Regarding the wrought iron rods, an actual slackness of some rods or a general reduction of rod sections due to corrosion could be a possible cause of decreased effectiveness of the vertical elements. Finally, local damage effects, which in general are more difficult to model, could be another cause of reduced stiffness or, alternatively, the truck weight may not have been exactly that stated by the driver.

The data contain some other anomalies. For example, in Figure 44, considering the L5U6 and L6U5 influence lines, the position of highest tensile force for the counterbrace and of highest compressive force for the main diagonal should be for load position L5 instead that L4. A similar anomaly was found for diagonal L7U6, although the experimental influence line of L8U7 was similar to the predicted one. These discrepancies may have occurred because the centroid of the truck was not measured, but estimated visually, and because the stopping points were not controlled precisely. Another possibility, one already discussed regarding displacements, is the local increase of stiffness caused by tightening rods L5U5 and L6U6, coupled with the relative slackness of the nearby vertical elements.

Figure 44 shows the axial forces in diagonal L6U5 as a function of load position, as measured on site (the measured strains were multiplied by the assumed modulus of elasticity and the section area of the element) and as predicted by numerical modeling. A different model, with only counterbrace L5U6 active, was used to simulate the actual condition of the bridge, since only vertical rods L5U5 and L6U6 were tightened. It can be seen that, at least for diagonal L6U5, the model correctly predicted the anomalous behavior experimentally observed.

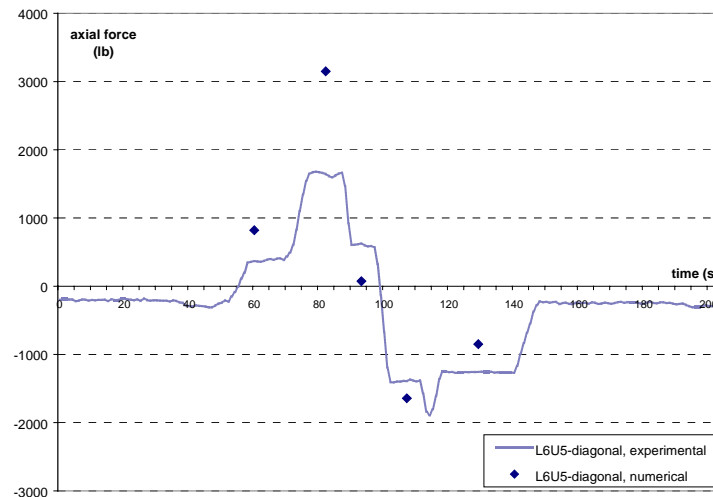


**Fig. 46: Experimental and numerical influence lines of diagonal L6U5. The numerical influence line has been obtained running a model with only counterbrace L5U6 active.**

## CONCLUSIONS

### Observations on the Static Behavior of the Pine Bluff Bridge

The numerical studies of the static behavior of Pine Bluff Bridge showed that the maximum axial stresses under dead load in the elements were less than 300 psi. Also, stresses from bending moment were an order of magnitude smaller than those from axial forces, and shear forces in the members were almost zero.

The maximum vertical displacements of the Pine Bluff Bridge under dead load were predicted to be 0.56 inch without the effect of the counterbraces, and 0.39 inch with the action of counterbraces. The analyses thus attributed a 28 percent increase of the bridge stiffness to the tightening of the rods and activation of the counterbraces, showing Howe's prestressing technique to be very effective.

The action of tightening a vertical rod primarily affects only the two adjoining panels, therefore all the rods must be pretensioned to assure a uniform behavior of the bridge. Prestressing caused an upward displacement of the truss, but it was small (0.06 inch), therefore, it would relieve only a small fraction of the dead load forces from the falsework, and it add a small camber to the bridge. Moreover, it is sensible to prestress a truss with the falsework removed and the dead load already active, to avoid a decrease of prestress in the counters once the falsework is removed. Tightening the rods at this time may, however, require more effort than would be needed with the falsework in place.

The maximum stresses due to a concentrated unit live load and a uniformly distributed unit live load on the half span were an order of magnitude lower than those produced by the effect of dead load alone. With a uniformly distributed live load of 40 lb/ft<sup>2</sup> on the entire bridge, the maximum compressive stress due to live and dead load was equal to 394 psi. It is not possible, however, to make a definitive statement on the reliability of the bridge from this evidence alone, because its strength could be controlled by the capacity of the joints.

Scaling the loads and using the influence lines of main diagonals and counterbraces, the minimum concentrated live load that would cause slackness in the diagonal elements of the truss was calculated. This live load was equal to 6.5 tons to loosen the central main diagonals with the counters inactive, and about 18 tons to loosen the counterbraces of the panels adjacent to the end ones with active counters. These values clearly show the improved behavior of the bridge when the counters were prestressed. The same two elements were loosened, in the two bridge conditions, for uniformly distributed live loads of 57 lb/ft<sup>2</sup> and 74 lb/ft<sup>2</sup> on the half span of the bridge. The live load used for country bridge design by the end of the nineteenth century for bridges with spans of about 100' was a 5-ton concentrated load and 70 lb/ft<sup>2</sup> of uniformly distributed load. Early nineteenth century builders may have used lower design loads.

Longitudinal wood shrinkage causes significant stresses in the elements and a considerable loss of prestress in the counterbraces. This happens because shrinkage is not uniform in all the truss elements; the iron rods do not shrink. At a value of shrinkage much smaller than 0.002, all the counters go slack and the truss reverts to the form of Model A. Further shrinkage would cause additional displacements but no further changes in forces. Shrinkage also causes downward displacements, of the same order of magnitude as those experienced under dead load. The effects of tangential and radial shrinkage at nodes cannot be evaluated without a three-dimensional model. When cast-iron bearing shoes with flanges are used, there is no bearing on the horizontal elements,

and their transverse shrinkage should not affect nodal displacements or element forces. In the Pine Bluff Bridge, the cast iron blocks have no flanges.

Creep produces a decrease of prestressing forces in the counterbraces, but it may or may not loosen them. Changes in forces due to creep are definitely smaller than those produced by shrinkage, and they are of the same order of magnitude of forces from prestressing. The first critical counters that may become slack are those closest to the span ends. However, to predict the time-to-slackness, a viscous stress-strain model for wood that takes into account the change in stresses with time is needed.

The shrinkage and creep analyses reported here, therefore, are useful only to give a qualitative description of the phenomena. They provide a general idea whether slackness will occur and where, but they cannot give more detailed information on time-to-slackness. It is evident that shrinkage and creep affect the structural behavior of the bridge, but periodic re-tightening of the nuts, more often during the early stages of the bridge's life, may be sufficient to maintain the bridge in proper conditions.

### **Observations on the Experiments and Comparison with the Numerical Analysis**

With a simple test, it was possible to evaluate the axial forces produced by tightening rods, the technique proposed by Howe. With this simple evaluation, the order of magnitude of the prestressing load that can be achieved in the vertical rods was determined to be about 12-13 kips, and it was possible to carry out structural analyses that properly took into account the prestressed state of the bridge. Experimental influence lines for certain element forces and vertical displacements were plotted, and they allowed an interpretation of the bridge's actual behavior. Anomalies in the influence lines of some diagonals were likely due to the local increase of stiffness caused by tightening only two adjacent rods.

Finally, some differences between the results of the numerical model used for the structural analysis of the Pine Bluff Bridge and those of the experimental tests were found. The actual stiffness of the bridge was 39 percent lower than that predicted by numerical modeling. This difference could be due to wood aging and decay, iron corrosion and rod slackness, or by the imprecise definition of the weight of the truck used for the experimental tests.

Qualitatively, however, the model described the truss behavior accurately. While they have certain limitations that arise from some simplifying assumptions, these linear elastic plane frame models can be useful for predicting the short-term behavior of wooden trusses, but they need to be verified and calibrated by experimental testing.